Lighting-up nanocarbons through hybridization: Optoelectronic properties and perspectives

Original
Lighting-up nanocarbons through hybridization: Optoelectronic properties and perspectives / Osella, S., Wang, M., Menna, E., Gatti, T.. - In: OPTICAL MATERIALS. X. - ISSN 2590-1478. - 12:(2021), p. 100100. [10.1016/j.omx.2021.100100]

Publisher:
Elsevier

Published
DOI:10.1016/j.omx.2021.100100

Optical Materials: X 12 (2021) 100100

Contents lists available at ScienceDirect

Optical Materials: X

journal homepage: www.journals.elsevier.com/optical-materials-x

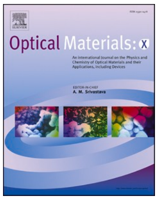

Invited Article

(INVITED) Lighting-up nanocarbons through hybridization: Optoelectronic properties and perspectives

Silvio Osella [a,**], Mengjiao Wang [b], Enzo Menna [c,d,***], Teresa Gatti [b,*]

[a] Chemical and Biological Systems Simulation Lab, Center of New Technologies, University of Warsaw, Banacha 2C, 02-097, Warsaw, Poland
[b] Center for Materials Research, Justus Liebig University, Heinrich-Buff-Ring 17, 35392, Giessen, Germany
[c] Department of Chemical Sciences, University of Padua, Via Marzolo 1, 35131, Padova, Italy
[d] Interdepartmental Centre Giorgio Levi Cases for Energy Economics and Technology, University of Padua, Padova, Italy

ARTICLE INFO

Keywords:
Nanocarbons
Carbon nanostructures
Photoactive nanomaterials
Nanohybrids
Optoelectronics

ABSTRACT

In recent years, a plethora of material systems have been designed and prepared to increase the performance of light harvesting and light-emitting technologies, and to develop new and attractive applications. Limitations of state-of-the-art devices based on organics (both conjugated polymers or small molecules/oligomers) derive largely from material stability issues after prolonged operation. This challenge could be tackled by leveraging the enhanced stability of carbon nanostructures (CNSs, including carbon nanotubes and the large family of graphene-based materials) in carefully designed nano-hybrid or nano-composite architectures to be integrated within photo-active layers, paving the way to the exploitation of these materials in contexts in which their potential has not been yet fully revealed. In this review, we discuss the theoretical and experimental background behind CNSs hybridization with other materials for the establishment of novel optoelectronic properties and provide an overview of the existing examples in the literature that allow to forecast interesting future perspectives for use in real devices.

1. Introduction

Nanotechnology provides an exceptionally rich platform to manipulate the multiple interactions of light with matter. The optical response at the interface of nanostructures can be fundamentally different from the bulk and can be optimally tuned by controlling shape, size and interactions at the nanoscale. The library of methods to produce nanostructures has witnessed a rapid development in recent years. In particular, the solution processing is a very versatile and promising approach in which colloidal inks of nanomaterials with specific properties are implemented to produce functional thin films [1]. The rational hybridization of pre-identified nano-objects [2–4] (the nano building blocks, NBBs) and their formulation into stable colloidal dispersions ready for thin films processing are essential activities to obtain functional devices [5,6]. The key to this development is the control of the interactions and self-assembly properties of the NBBs at the nanoscale, achieved through a rational interface design, in order to optimize the structure-property-function relationships in the integrated nano-systems.

By taking advantage of the unique properties of low-dimensional materials, it is possible to assemble the NBBs into hybrids employing a bottom up approach [7,8], to gain control over the different degrees of complexity of the individual structures and to fine tune the optoelectronic and transport properties of the final assemblies, in an attempt to mimic the perfection of natural architectures such as Photosystems I and II in plants and bacteria [9]. The presence of highly interchangeable NBBs might allow the synthesis of the best assembly for a given target function, i.e. obtaining of smart materials which pertain to Type I (energy transfer-ET) or Type II (charge transfer-CT) heteronanojunctions (HNJs). Moreover, the rational design ensured by the use of the state-of-the-art computational methods [10,11] might constitute the base for a pre-screening of many different NBBs combinations to perform the fine tuning of the energy levels and of the interface energetics, together with a mechanistic insight into the ET and CT processes occurring within these HNJs.

The interest in 0/1/2D carbon nanostructures (CNSs) has been

---

* Corresponding author.
** Corresponding author.
*** Corresponding author. Department of Chemical Sciences, University of Padua, Via Marzolo 1, 35131, Padova, Italy.

E-mail addresses: s.osella@cent.uw.edu.pl (S. Osella), enzo.menna@unipd.it (E. Menna), teresa.gatti@phys.chemie.uni-giessen.de (T. Gatti).

https://doi.org/10.1016/j.omx.2021.100100
Received 19 August 2021; Received in revised form 6 September 2021; Accepted 6 September 2021

consistently high over the last two decades, due to their outstanding electronic, thermal, optical, chemical and mechanical properties. Their beneficial effects in optoelectronics, photovoltaics and sensing have been amply demonstrated [12–15]. However, their use in devices has been mainly limited to the realization of (semi)transparent electrodes as replacement of the brittle and relatively expensive indium tin-oxide (ITO) or for incorporation into ancillary layers. Incorporation of CNSs within photoactive layers has only been given marginal attention up-to-now, despite their expected advantages. Due to the extended (semi-2D) π-electron system, and thus greatly "stabilized" frontier energy levels (highest occupied molecular orbital-HOMO, and lowest unoccupied molecular orbital, LUMO) some of these CNSs are indeed characterized by a better "chemical" robustness relative to "standard" conjugated small molecule organic semiconductors (SMOSs) and polymers, while retaining flexibility and light-weight. In addition, the development of CNS-based light absorbers and emitters in the last ten years, i.e. the graphene quantum dots (GQDs), is contributing significantly to the realization of CNS-based photoactive layers [16]. However, fostering key optoelectronic processes in *ad hoc* designed carbon-based structures, i.e. the production of an electric current following light absorption and/or the opposite process (namely electroluminescence – EL -), by means of efficient transfer of energy and/or charges at binary interfaces between low dimensional materials is still the main challenge.

This challenge can be targeted in some cases by implementing CNSs hybridization with specific light harvesting/emissive NBB units, such as in the donor-acceptor (D-A) dyads [17–20]. The different NBBs can be responsible for the following processes: 1) efficient light harvesting; 2) efficient charge separation; 3) efficient light emission. To have an efficient current generation, the 0D, 1D and 2D NBBs have to be conveniently assembled with tight control over the kinetics, space and energy variables. A successful design strategy takes-into-account the use of light harvesting components able to generate long-living excitons which efficiently separate into holes and electrons and emissive components characterized by high PL quantum yields (PLQY) and PL lifetimes (*kinetics dimension*). In addition, to obtain a highly efficient charge separation, the photogenerated charges have to be separated in space in order to avoid charge recombination (*space dimension*) and the energetics have to be controlled by the redox potentials or work functions of the NBBs (*thermodynamics dimension*), to assure the unidirectionality of charge flow and a high current output yield. Control over light emission processes can be instead carried out by tuning of valence/conduction bands and/or HOMO-LUMO positions so as to favor ET. By implementing well-designed hybrid structures, some of the major bottlenecks of heterojunctions to date might be tackled, focusing on achieving the key features like: 1) an efficient light absorption/emission; 2) an efficient CT/ET; 3) a low recombination of photogenerated charge carriers; 4) an excellent environmental and photo-stability; 5) a nanoscale control over interface geometries and properties.

In this review, we will highlight the major contributions in the field of CNSs hybridization with optically active NBBs from both the organic and inorganic nanomaterials realm, targeting the utilization in optoelectronic devices such as light-emitting diodes (LEDs), solar cells, photodetectors and sensors, but also for other light-conversion processes such as photocatalysis/photoelectrochemistry. The aim is to stimulate further research in this field until now relatively poorly explored, by revealing the hidden potential for application in future low-cost, lightweight and portable technologies such as those nowadays extremely relevant for the internet of things (IoT) [21,22].

2. Carbon-based NBBs

CNSs offer a unique advantage for a wide variety of energy/optoelectronics-related technologies, since the confinement of charge carriers to nanoscale dimensions can lead to distinctive optical and electronic properties, especially near or below the Bohr radius (which defines the typical Coulomb electron–hole distance in a material) [23–26]. These quantum effects arise in materials confined in 2D (with the large family of graphene-based materials - GBMs), 1D (including single and multi-walled carbon nanotubes -SWCNTs/MWCNTs and graphene nanoribbons - GNRs) and in 0D (the GQDs). Different quantum confinement effects exist, but some of the most important for photo-responsive energy conversion materials are: 1) size-tunable electronic and optical band gaps; 2) possible ultra-high charge carrier mobilities, in some cases approaching the ballistic limit; 3) strongly different kinetics for excited-state processes relative to bulk; 4) symmetry-dependent optical selection rules. The different CNSs are here briefly recalled based on their specific dimensionality (Fig. 1), and their peculiarities underlined.

0D CNSs. GQDs are environmentally friendly and lower-cost counterparts of inorganic semiconductor quantum dots, being free of toxic and/or precious metals. In materials science, most of the GQDs are produced by "cutting" graphene through top-down methods or hydrothermal treatment of small aromatic hydrocarbons or other organic molecules, but it is not possible to precisely control the structures and properties of the resulting GQDs by such methods [27,28]. By changing the size, shape and edge structure, GQDs with desired energy gaps and absorption ranges can be obtained [29]. By combining several different GQDs with complementary absorption profiles, it is also possible to achieve broad optical absorption from the UV to the visible and near IR range. The key advantage of GQDs as chromophores for light energy harvesting is their extremely high thermal and photostability, thanks to the rigid carbon frameworks with strong aromatic stabilization and delocalization of π-electrons over the planar cores [30]. Furthermore, GQDs can also be coupled or even fused with other organic chromophores (such as SMOSs), inducing unique optoelectronic properties, such as broad absorbance and white light emission [31,32]. GQDs show great promise due to their high light absorption coefficient and luminescence, chemical stability, low photo-bleaching, efficient dispersibility in solvents for solution processing, low environmental impact and moderate costs of production [33]. While the majority of GQDs are fabricated via top-down methods, it is also possible to bottom-up synthesize GQDs with *ad hoc* properties (Fig. 2) [29]. Such materials can be functionalized with many different functional groups (Fig. 2) in order to tailor their optoelectronic properties, accommodate multiple charge carriers and graft them to surfaces or to other molecules/nanostructures. The design of electron-rich derivatives can be addressed through the addition of electron-donating groups on the periphery of the GQDs [34–36]. Several holes can be accommodated on the large aromatic core, and additional functional groups may guest more holes (e.g., through the addition of multiple pyrrole rings which can accept one hole each) [34]. The charges are delocalized over the extended aromatic cores, making the reactivity low, and, thus, their stability high compared to smaller molecules. An important aspect of such materials is that different structures can be synthesized in which the energy levels can be precisely tuned by changing the molecular size, shape and edge structures, which allows the study of the CT mechanism. Moreover, the bottom-up synthesis allows for the heteroatom-doping of the GQDs with nitrogen, oxygen, sulfur, boron, and also other heteroatoms, which enables fine-tuning of the energy gaps and levels of the GQDs [37].

1D Materials. SWCNTs have unique optoelectronic properties and represent one of the most direct realizations of 1D electron systems available for fundamental studies today, attracting much theoretical and experimental interest. As research into purification of their different forms within a mixture towards obtaining chirality-enriched samples continuously improves, with commercially available purely semiconducting species (such as 6,5 or 7,6) being present on the market for use in basic research, the studies on their incorporation into thin films technologies are made easier and can provide reproducible outcomes [38–41]. Also, with SWCNTs as with other CNSs, functionalization stands out as tool to modulate the optoelectronic properties (but also spins, as can happen with the brightening of trions in functionalized SWCNTs) in a wide spectral range [42–45]. Exohedral organic

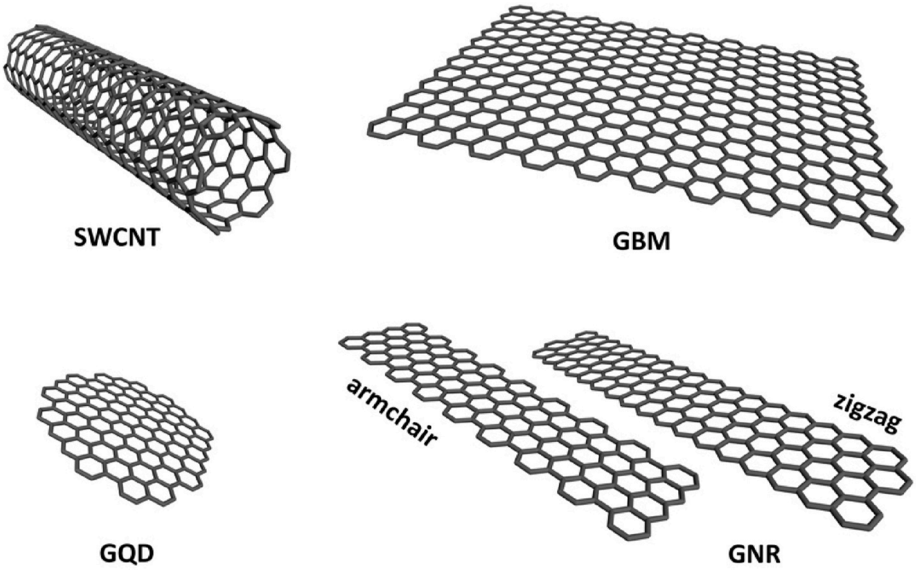

Fig. 1. Sketches of the structures of the different CNS examined in this Review. From top-left, clockwise: single walled carbon nanotubes (SWCNTs), graphene-based materials (GBMs), graphene nanoribbons (GNRs), graphene quantum dots (GQDs).

functionalization is carried in engineered stable suspensions to ensure homogeneous distribution of functional groups on the CNS surface [46,47]. Coupling of SWCNTs with 0D materials such as SMOSs might pave the way to hybrid architectures able to optically modulate conduction or to feature improved light emission in the NIR as a result of ET. Given the large variety of functionalization strategies (at surfaces, at edges) [48] and of possible nanomaterial combinations, the field is undoubtedly still rather unexplored and deserves higher attention of both theoreticians and experimentalists.

When graphene is cut along a specific direction, a strip with a nanometer sized width ($<$10 nm) is obtained, which is referred to as a GNR [49–51]. Compared to graphene, GNRs show distinctive features in their electronic structure and optical properties, such as the opening of a finite band gap, which makes them attractive materials for carbon-based nanoelectronics [52,53]. The geometrical arrangement of carbon atoms at the periphery, the passivation of the end carbon atoms with hetero-atoms (i.e. hydrogen, halogens), and the finite width of the GNRs strongly affect their electronic properties. Both theoretical and experimental studies have demonstrated that the electronic and magnetic properties of GNRs are critically dependent on their widths and edge topologies [54]. These confinement effects yield an increased band gap in armchair edge nanoribbons (ANRs) that behave as semiconductors. ANRs feature band gaps that scale inversely proportional to the ribbon width and are highly sensitive to the number of armchair chains across the ribbon [55]. GNRs delineated with zigzag edges (ZNRs) are typically metallic because of the spin-ordered states at the edges, with those states localized near the Fermi level; nanoribbons with a higher fraction of zigzag edges exhibit a smaller band gap than a predominantly armchair edge ribbon of similar width [56]. In addition, cove-edged GNRs with unique curved geometry are attractive because they can exhibit improved dispersibility in solution and provide an additional means to control the optoelectronic properties of GNRs [57]. Those peculiarities have raised the interest of scientists for the design, synthesis, and electrical characterization of GNRs. Finite widths combined with periphery effects also provide GNRs with peculiar opto-electronic and transport properties.

2D Materials. GBMs have attracted a worldwide attention due to their unique structures, excellent physical and chemical properties [58] since Geim and Novoselov et al. first reported graphene in 2004 [59]. The structure of these materials is layered, stacked by van der Waals interlayer forces. The surface is without dangling bonds, leading to an easy assembly into a variety of ultrathin layered materials without considering lattice mismatch [60]. In the past 10 years, also other versatile 2D materials have been explored evolving from graphene with zero band gap to a non-zero band species [61]. GBMs have been proven to possess distinctive physical characteristics. For example, single layer graphene exhibits unique electronic and transport properties, such as linear dispersion of both valence and conductive bands at the high-level symmetry K point, which translates into extremely high charge carrier mobility, up to 50,000 cm^2/V. In addition, it has a high surface area and is very flexible and transparent. Thus, coupling graphene with light harvesting molecules can be a way of improving both ET and CT processes at the interfaces [62]. Due to presence of either structural defects or doping, their peculiar electronic property can vary, which in turn can lead to a change in their energy level alignment resulting in a decrease of the energetic barrier for transfer processes, making them ideal candidates to obtain Type I or Type II HNJs in combination with the right chromophores. In addition, their unique electron-rich structure makes them good electron acceptors, and contribute to spatially separate the photogenerated charges from the chromophore. Their high specific surface area is extremely beneficial when the generation of multiple charges is considered. The coupling of 2D-0D materials might strongly increase the CT processes due to specific interactions and transfer states established at the hetero-interface which might also be responsible for the stability of the derived assembly.

3. CNSs hybridization for use in optoelectronic devices

The fine tuning of the frontier energy levels of the NBBs at the interface can lead to two distinct types of HNJs, namely Type I and Type II. The difference in these HNJs is translated in different transfer mechanisms of action. In fact, while for Type I HNJs ET prevails, foreseeing use in EL application, in Type II the CT prevails, with potential application in devices in which light energy is converted into an electrical current (Fig. 3).

HNJs formed by combining different CNSs with other NBBs offer a unique platform that can reap the benefits of the combined low dimensional material systems. Pairing these disparate systems can not only lead to new nano-assemblies that are highly absorptive/emissive with exceptional mobility, but also enable control over bandlike to charge-hopping transport. However, energy dynamics at HNJs associated with Frenkel excitons in confined systems such as 0/1D and

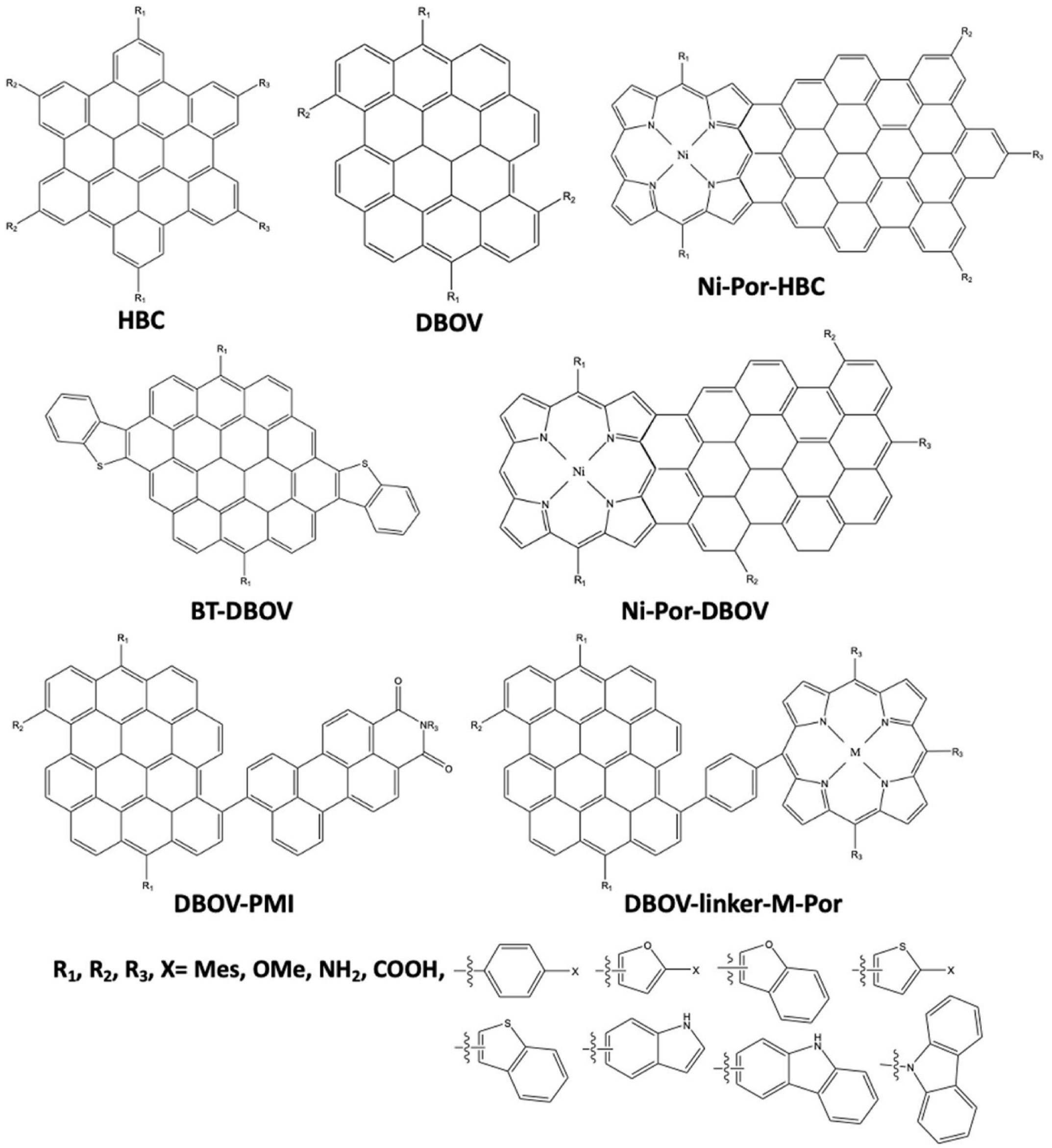

Fig. 2. Examples of molecular structures of bottom-up synthesized GQDs and of the different peripheral substituents that they can feature.

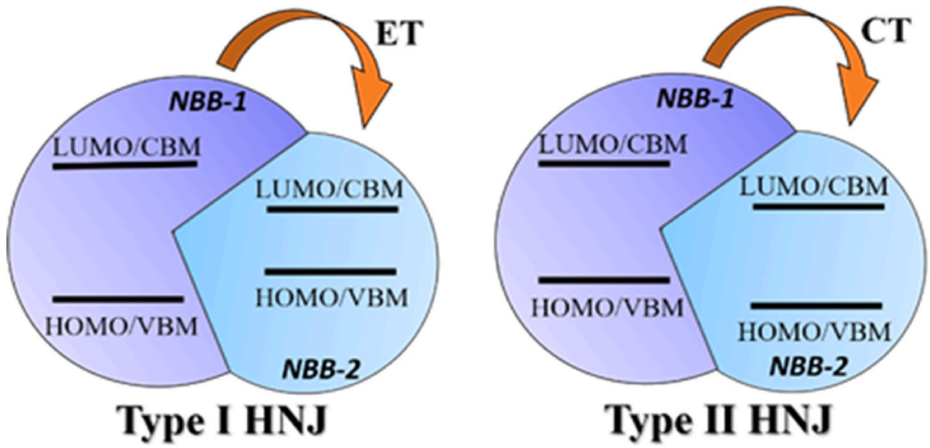

Fig. 3. Energy landscape and transfer processes in Type I and Type II HNJs.

Wannier–Mott like excitons in 2D materials, remain a rather hitherto unexplored area of investigation [63]. Moreover, HNJs offer a unique platform to study unknown rich physics associated with ET/CT processes and could open a plethora of applications ranging from biochemical sensing, ambient lighting, and photovoltaics beyond commonly used devices, to pave the way to the future creation of many fit-for-purpose heterostructures [64].

CNSs can thus have great potential for integration in optoelectronic devices to convert light into an electrical current (solar cells, photodetectors) [64,65] and to perform the opposite function, i.e. EL (light emitting diodes), as substitutes of SMOSs/conjugated polymers or in combination with these last ones to boost their properties and stability. For what concerns EL, while current visible-range organic light emitting diodes (OLED) technology is at a mature stage of development, with commercial uses in the display and lighting industry, OLEDs emitting further in the NIR (at wavelengths beyond 800 nm) would facilitate a range of new applications, in particular medical bioimaging and skin treatment as well as in optical data communication and night-vision devices [66]. CNSs can again be helpful in this regard and pave the way to the realization of efficient and stable NIR-OLEDs. The first demonstration of a NIR-OLED based on semiconducting mono-chiral (6, 5) SWCNT was already reported [67]. The external quantum efficiency of these devices was maximized only up to 0.014%, thus leaving ample room for improvement, e.g. via the optimization of the EL layer. A recent literature perspective on SWCNT highlights the future promise of these systems [68]. One valuable possibility to improve NIR-PLQY of SWCNTs in the NIR consists in covalent chemical functionalization generating sp^3 defects acting as luminescent exciton traps, and this strategy has been very recently employed to produce large quantities of defect-tailored SWCNTs enabling aerosol-jet printing and spin-coating of thin films with bright emission almost free from re-absorption [69,70]. Moreover, recently it has been observed that also GNRs in a twisted, non-planar conformation can absorb/emit light in the NIR and possess a high intrinsic charge carrier mobility (up to 600 cm^2/Vs), making them promising candidate for optoelectronics [71,72].

3.1. CNSs-based nanohybrids with organic NBBs

Modifications of the organic network in CNSs can allow access to efficient coupling with other CNSs or SMOSs, thus producing new functional nanohybrid architectures with novel promising properties [73]. Hybrids of dyes and photochromic molecules with GBMs have been used to enhance or modulate photocurrents (also as a function of the irradiation wavelength) in several configurations, paving the way to the fabrication of light-responsive devices for application in optoelectronic or energy-related devices where efficiency can be addressed by controlling ET/CT processes happening at the HNJs [74–77]. However, the combinations of SMOSs with CNSs having fundamentally different dimensionalities remain very challenging and require a powerful combination of design and synthetic/functionalization skills to provide species with well-defined shapes and controlled properties.

Covalent and non-covalent approaches can be used to generate nanohybrids based on CNSs, relying on chemical strategies (commonly used techniques are amide/ester linkages and diazonium grafting) or π-stacking interactions with the CNS surface [78,79]. In addition, following tailored surface functionalization of a given NBB, approaches towards nano-hybrids formation can be further distinguished as grafting-to and grafting-from [4,80].

Covalent functionalization of CNSs with photoactive species affords stable derivatives and allows to tune not only optoelectronic properties, but also processability [81,82]. D'Este et al. reported a co-functionalization approach to graft both a fluorescent dye and a solubilizing moiety (polyethylene glycol, PEG) through formation of amide bonds on partly oxidized SWCNTs [83]. The choice of different dyes led to a range of photophysical behaviors, from a strong photoluminescence (PL) quenching in the case of fluorene to an almost preserved PL for anthracene [84]. At the same time, PEG chains provided excellent solubility and hampered aggregation of the tubes, thus allowing a detailed investigation of exciton recombination dynamics.

Some of us reported in 2017 on the synthesis of a covalent nanohybrid between reduced graphene oxide (RGO) and a prototypical organic donor-acceptor dye (Fig. 4a), used as photosensitizer for high band gap semiconductors such as anatase TiO_2 in dye sensitized solar cells (DSSCs) [85]. This hybrid was demonstrated to ensure a good photovoltaic response to DSSCs that featured it as photosensitizer, but, more remarkably, it allowed an improvement in device stability, due to the tighter binding of the nano-hybrid photosensitizer to the titania surface compared to the reference free dye. In addition, electron paramagnetic resonance studies proved that the presence of the covalently bound RGO slows down charge recombination at the dye-titania interface, thus limiting one of the most detrimental process for the device performance [86].

A further step ahead into the engineering of nanocarbon-SMOS nanohybrid structures, regards the development of a cross-linking synthetic strategy involving two components, namely bithiophenediketopyrrolopyrrole (TDPP) oligomers and few layers graphene flakes (obtained from the liquid exfoliation of a graphite via shear-mixing) [87] to produce a cross-linked composite (c-EXG-TDPP, Fig. 4b). The cross-linking approach provides a blue colored hybrid material with impressively high solubility in common organic solvents and excellent film-forming ability (Fig. 4c), with sharp difference from the case of the not-cross-linked species (which behaves more like pristine graphene, thus with a general tendency to form aggregate structures when deposited from liquid dispersions onto common transparent substrates like glass or ITO). PL quenching is not homogeneous within the film, but it results more pronounced in the areas of the thin film where graphene flakes are allocated (Fig. 4d). Preliminary data obtained from ultrafast pump-probe spectroscopy indicate that the observed PL quenching of the TDPP moieties is due to a photo-induced CT process between the dye and graphene occurring on the sub 50 ps timescale [88]. This process appears to be much more efficient and faster in the cross-linked nano-hybrid compared to the reference not-cross-linked one.

As a drawback of covalent approaches, it must be noted that they induce the formation of sp^3 defects on the CNS structure, which might affect electronic and transport properties. For this reason, controlled synthetic protocols, such as flow chemistry [90], are highly desirable to limit the density of functionalization with a trade-off between beneficial properties of the grafted molecules and unwanted degradation of the CNS [91].

SWCNTs peculiar structure allows to encapsulate molecules inside their cavity, to obtain endohedral derivatives often called nanotube peapods. Indeed, the first species encapsulated in SWCNTs were fullerenes [60], affording hybrids with a shape resembling a pod full of peas [92]. Endohedral functionalization, being based on non-covalent interactions, does not introduce defects in the nanostructure and preserves its sp^2 carbon lattice, responsible for the unique electronic and optical properties. On the other hand, the encapsulated molecules are arranged in a confined space, aligned along the axis of the nanotube and surrounded by the sp^2 carbon structure, granting stable π-π interactions in the case of conjugated molecules. In fact, while π-π interactions with the outer walls of SWCNTs can be exploited to obtain exohedral photoactive derivatives [93–95], the stability of such complexes is much lower and strongly affected by the surrounding environment (e.g. solvent and concentration of the solution) compared to endohedral hybrids. These premises make the preparation of peapods with photoactive molecules an appealing approach to study their PL properties. Moreover, light emitting nanotube peapods disclose opportunities to couple the electronic properties of the nanostructure with the optical properties of the molecules, in view of applications such as sensing, photonics and quantum communication.

Strategies for the encapsulation rely on the diffusion of the molecules either in the gas phase or in solution. Vapor phase encapsulation is

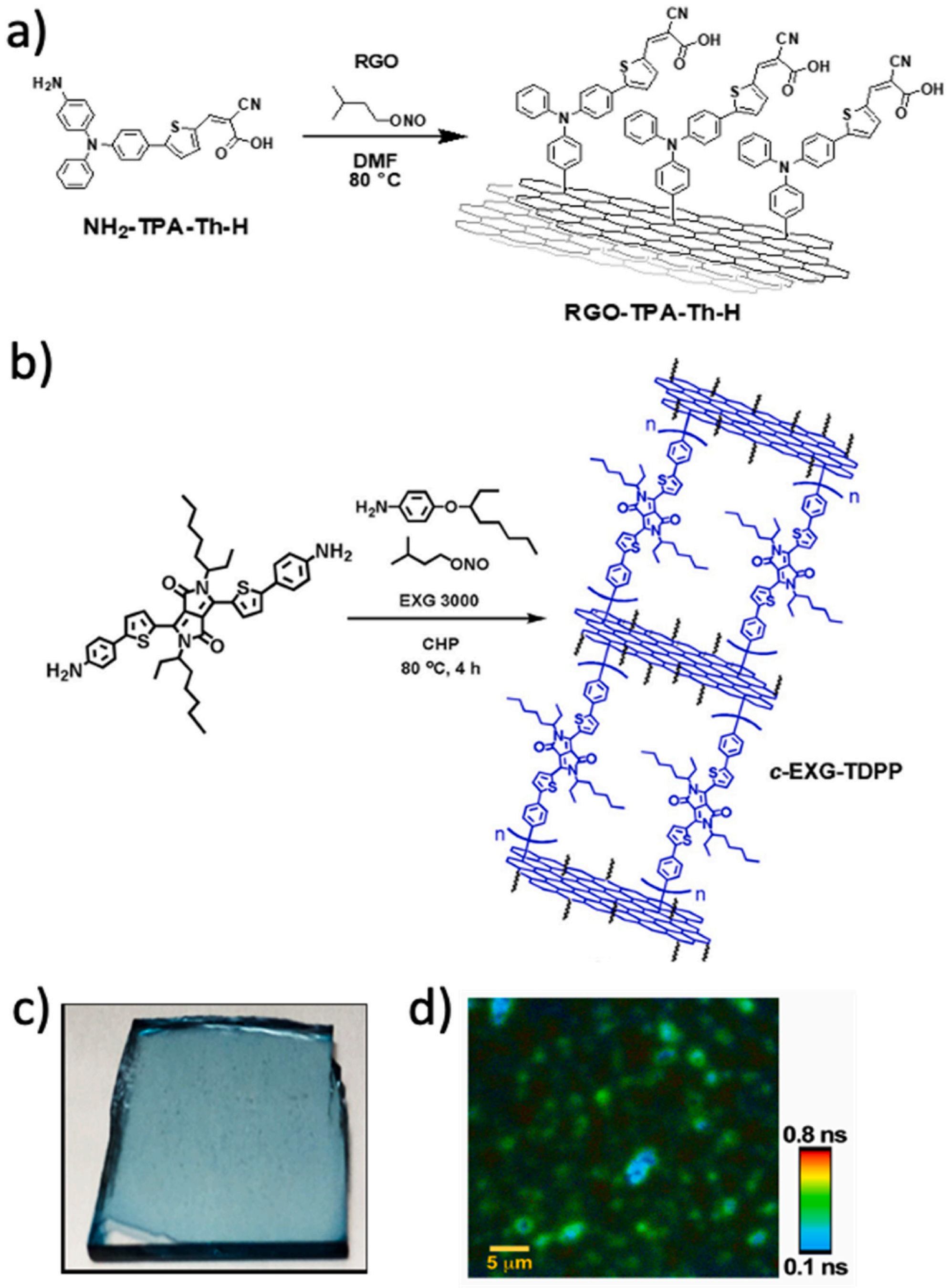

Fig. 4. Examples of photo-active CNSs-SMOSs covalent hybrids. a) Synthetic route towards an RGO-organic dye hybrid used as photosensitizer in a DSSC. Reproduced from Ref. [85] with permission of Elsevier. b) Synthesis of a cross-linked graphene-organic dye blue hybrid with outstanding film-forming ability c). Map of the PL lifetimes within the blue film showing areas where PL quenching is more pronounced being coincident with the local presence of graphene flakes. Adapted from Ref. [89] with permission of Elsevier. (For interpretation of the references to color in this figure legend, the reader is referred to the Web version of this article.)

achieved, when possible, by heating molecules under vacuum. Alternatively, to avoid thermal degradation, SWCNTs can be dispersed in a solution of the molecules to be encapsulated and kept under reflux [96]. It has been pointed out that viscosity and surface tension can hamper diffusivity of molecules and for this reason the use of supercritical carbon dioxide has been proposed instead of conventional solvents [97]. Also in this case, operating temperature (typically around 50 °C) is mild enough to avoid degradation of labile molecules or functional groups, thus widening the range of candidate structures for the encapsulation. Efficient endohedral functionalization obviously requires open access to the inner cavity of SWCNTs, therefore preliminary purification and annealing processes, opening ends and removing impurities and carboxylic or other functional groups, are crucial.

The structure of photoactive organic molecules is often characterized by aromatic rings and extended π-conjugated systems that may establish hydrophobic and π-π stacking interactions with the outer walls of CNSs. For this reason, thorough washing procedures of peapods, until no traces are found in the solvent, are required to make sure that the only molecules left in the sample are those inside SWCNT cavities. A purification approach to remove non-encapsulated molecules based on controlled sublimation (dynamic vacuum washing) was also proposed [98].

In 2010, Loi et al. reported the encapsulation of conjugated oligomers inside SWCNTs to obtain peapods emitting visible light, hence interesting photon sources to study future materials for optoelectronic devices [99]. The endohedral functionalization of SWCNTs with α-sexithiophene (6T) was achieved through sublimation (Fig. 5a) and demonstrated by means of HRTEM and optical spectroscopy.

Interestingly, HRTEM images of 6T@SWCNT peapods show that 6T molecules inside the tubes tend to align in two parallel chains 0.4–0.8 nm apart, depending on the tube diameter, with a molecule-tube

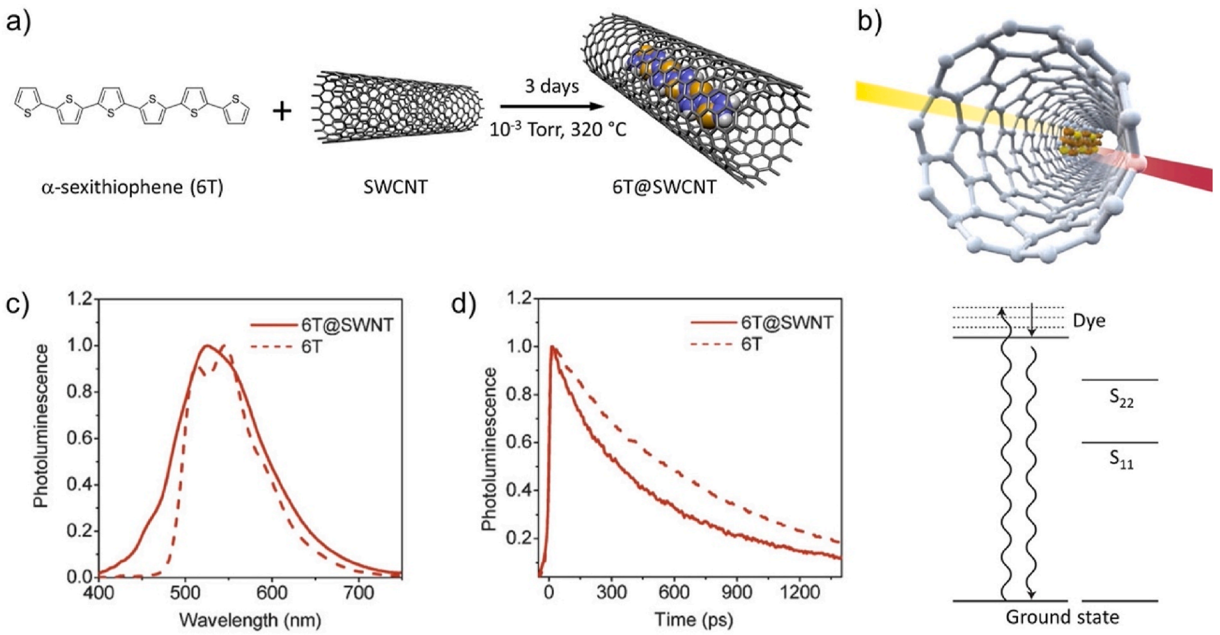

Fig. 5. a) Endohedral functionalization of SWCNTs with sexithiophene to obtain 6T@SWCNT peapods; b) emission occurs from the encapsulated 6T dye, without energy transfer to the lower S22 and S11 levels of the SWCNT, reproduced from Ref. [100] with the permission of Macmillan Publishers Limited. c) Photoluminescence spectra of 6T and 6T@SWNT and d) PL decays of 6T@SWNT and 6T at 515 nm, reproduced from Ref. [99] with the permission of Wiley.

distance in the range of 0.32–0.35 nm. DFT calculations support stability of such an arrangement for the range of diameters of the SWCNT employed (1.2–1.5 nm).

Encapsulation of 6T affects Raman features of molecules (such as a shift for some bands and a new one appearing) and tubes (a shift of 5 cm^{-1} for the radial breathing mode bands), while interactions between pea and pods leads to a red shift in the absorption features of 6T. Similar results were obtained with shorter oligomers α-quaterthiophene and α-quinquethiophene [98]. Steady state and time-resolved PL measurements (Fig. 5c and d) show that 6T retain an efficient emission in the visible spectral range upon encapsulation, with a limited quenching that induces a faster decay of PL (lifetime, $t = 563$ ps) compared to the free molecule in solution ($t = 813$ ps). As it has been highlighted by Kataura and Yanagi [100], the hybrid emits light from an excited state of the dye molecule, instead of going through a decay to the lowest excited state (S_{11}) localized on the SWCNT, thus violating Kasha's rule (Fig. 5b). Such a behavior, probably due to a mild interaction between 6T and SWCNT, allows the emission at shorter wavelengths (550 nm) than a SWCNT would usually do, disclosing interesting perspectives for optoelectronic devices. In consideration of the interest for electroluminescent materials, further investigations based on PL experiments and DFT calculations provided evidence of stronger interactions between peas and pods in the excited state and in particular suggested that applying a voltage to the SWCNT would enhance light emission of the molecule [101].

Moving from these first reports, a number of investigations on photoluminescent nanotube peapods filled with sexithiophene [102–105], and other thienyl oligomers [106–113] have appeared in the literature. Thanks to those works, together with others based on different classes of conjugated organic chromophores encapsulated in SWCNTs [114–120], a quite clear picture can be drawn of general properties of photoactive endohedral hybrids, and how they can be modulated by choosing the dye structure or the nanotube size. Different works, through Raman and TEM investigations, confirm that the arrangement of the molecules inside the tubes depends on the SWCNT diameter and encapsulation conditions [103,106,107], and how this in turn affects optoelectronic processes like charge and energy transfer [108,111,116]. In particular, energy levels of frontier orbitals, hence electronic transitions and related photophysical behavior, are strongly affected by the size of the nanotube cavity, as confirmed by DFT calculations [113]. In view of applications such as biomolecular imaging, materials with a large Stokes shift are appealing for the related enhancement of PL quantum yield. As shown by Iijima and coworkers in the case of perylene, encapsulation in a SWCNT allows to obtain dimers with a controlled arrangement leading to a large Stokes shift and increased emission lifetimes, avoiding undesired spectral broadenings [115]. The selection of semiconductive SWCNTs encapsulating photoactive molecules like squaraine derivatives, can strongly enhance the possibility to tune PL and electronic properties of the hybrids, as reported by Blackburn and coworkers [119]. Characteristic but weak IR absorption of SWCNTs is also influenced by the interactions with thienyl oligomers, which may have relevant consequences in the emission behavior of hybrids, as highlighted by Bantignies and coworkers [109]. They in particular found fundamental differences in the effects of non-covalent interactions both outside and inside the tubes.

Tuning of PL properties can be further pushed through chemical modification of the dyes after their encapsulation, as demonstrated with the thermal fusion of pyrenes, by Fujimori and Urita [114], and of perylenes to obtain quaterrylenes, by Nakamura and coworkers [116]. The extension of encapsulated π-conjugated systems can be further increased up to polymer chains through similar thermal fusion approaches, as reported by Shinohara and coworkers and obtained not only for polythiophene [112], but also for coronene polymers inside SWCNTs [118].

As for the encapsulation strategy, besides vapor phase diffusion, some researchers focused on alternative approaches with encouraging results, such as the above-mentioned use of supercritical CO_2 that prevents the risk of thermal polymerization, as shown by Cadena at al [102]. From this point of view, an original approach was proposed by Fagan and coworkers, who efficiently encapsulated several different species from liquid phase, starting from neat dye samples [117]. They afforded some strongly luminescent hybrids and, once again, observed how the combination of molecule and tube size affects the properties of the peapods.

From a computational point of view, the creation of interfaces with different dimensionalities poses a series of challenges which can be overcome by the use of a multiscale computational approach, in which different length and time scales are considered for the description of different mechanisms. In particular, molecular dynamics (MD) simulations are commonly used to study the stability of the interfaces at the nm length scale, while only a small portion of the full systems is then considered for the CT mechanism, considered at the quantum mechanics/molecular mechanic (QM/MM) level of theory, in which only the pairs of molecules involved in the CT are considered at a high level of computation while the environment is considered as point charges (in the first approximation). A common strategy is thus to create a big slab of the interface (i.e. graphene with physisorbed or chemisorbed small molecules, for a 0D-2D interface), equilibrate it at the MD level and then cut out a small portion of it to compute the CT/ET mechanisms. The first approach towards this end is to study the shift in the work function (WF) of the conducting material (like graphene) upon the formation of the interface. This gives an accurate estimation of the change in hole/electron injection barriers and thus, the ease of transferring charges from one side to the other of the interface. From a computational point of view, two main contributions are responsible of the total shift in the WF: the first arises from the dipole moment of the molecular backbone of the molecule ($\Delta\Phi_{\mathrm{SAM}}$) and the second from the interfacial electronic reorganization upon physisorption (or chemisorption) of the molecules on the metal surface, namely the charge transfer contribution ($\Delta\Phi_{\mathrm{CT}}$, or bond dipole BD when chemisorption is present). Only when a permanent dipole moment is present in the self-assembled monolayer (SAM) the shift in the WF is observed.

An interesting system which comprehends both light absorption and CT ability is the interface consisting of pyrene-nitrilotriacetic acid-Ni^{2+}-imidazole molecule (pyr-NTA-M-IM) physisorbed on a graphene monolayer, in which a fine tuning of the CT abilities (magnitude and direction) can be obtained by changing the coordinated metal atom (Fig. 6) [121,122].

The calculated WF shift for the whole interface is equal to 1.34 eV, 0.44 eV and 1.16 eV for SLG/pyrNTA-Co-IM, SLG/pyrNTA-Ni-IM and SLG/pyrNTA-Cu-IM interfaces, respectively. To gain a deeper insight into the different contribution governing the WF shift, two different effects can be distinguished. First, the $\Delta\Phi_{SAM}$ contribution for the Ni containing interface is much stronger compared to the assemblies with Co^{2+} or Cu^{2+} cations, despite the smaller computed dipole moment. Second, while for Co^{2+} and Cu^{2+} the $\Delta\Phi_{SAM}$ and the $\Delta\Phi_{CT}$ contribution act to enhance the total WF shift, the presence of Ni^{2+} inverts this trend, leading to the smaller total calculated WF shift. As a result, different directionalities of the charge flow were observed arising from the different nature of the metal center (radical species or closed shell system) which, in turn, determines the energy level alignment at the interfaces.

A similar multiscale procedure has been applied to more complex interfaces considering a photoswitchable molecule adsorbed on graphene in which the functionality is increased, since an ‘on/off’ effect is present [74,75]. The molecule in question is an azobenzene derivative in which a long alkyl tail is added to enhance the interaction with graphene and the head modified with fluorine groups (Fig. 7).

From MD simulations, the authors predicted the formation of an amorphous monolayer of azobenzene derivatives physisorbed on a graphene sheet and extracted a statistical distribution of the dipole moment along the normal to the graphene sheet (which in turn affect the WF ability of the interface). To enhance the statistical significance of the computed WF, different representative molecules from the MD ensemble were considered in the QM/MM calculations. For the trans isomer, the accumulation of partial charge does not depend on its dipole moment, with a (small) partial positive charge present on the adsorbed molecule, indicating that graphene is slightly n-doped. The same conclusion holds true for the cis isomer. For both isomers of (fluorinated) azobenzenes, the CT contribution is negative and constantly independent of the molecular conformation and positioning on the graphene layer.

The second type of interfaces which are of interest consider the transfer of energy from one NBB component to the other (type I HNJs). By using low-dimensional materials, the interaction between electrons and holes becomes substantial and excitonic effects arising from the electrostatic interactions between photoinduced electrons and holes lead to interesting photoexcitation processes which are not seen in bulk materials [123]. One of the most interesting is the formation of exciton bound electron-hole pairs, which determine the yields of charge carriers and the mechanism of energy transport. Uncovering the impacts of excitonic effects on CNSs-based nanohybrids will not only give insights into photo-activated mechanisms but also pave new avenues for pursuing optimized solar energy utilization [124]. To describe this process from computation, two main approaches are considered in literature: multiscale approach via QM/MM methods and non-adiabatic molecular dynamics (NAMD) simulations. While the first can be applied to large interfaces and with different degree of accuracy depending on the description of the environment, the second allows for the depiction of the time evolution of the ET mechanism, but its computational cost limits its usage to relatively small systems.

With the QM/MM approach it is possible to investigate the origin of disorder in organic semiconducting materials forming 0D-0D interfaces, since the density of states (DOS) are directly accessible from the calculations. Furthermore, insight into the formation of the energy landscapes of the transport states are not easily accessible from experiments, but are essential for a rational design of efficient organic solar cells and organic light-emitting diodes [125]. The influence of interfacial disorder on ET

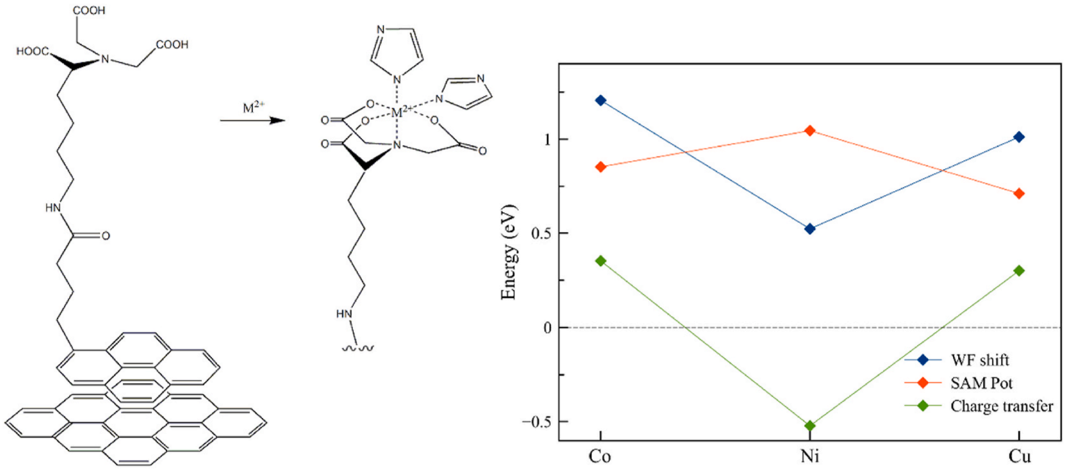

Fig. 6. *Left* Chemical structure of the graphene/SAM interface studied. $M^{2+} = Ni^{2+}$, Co^{2+} and Cu^{2+}. *Right* WF shift and contributions to it for three different interfaces. Adapted from Ref. [121] under the terms of the Creative Commons Attribution-NonCommercial 3.0 Unported Licence.

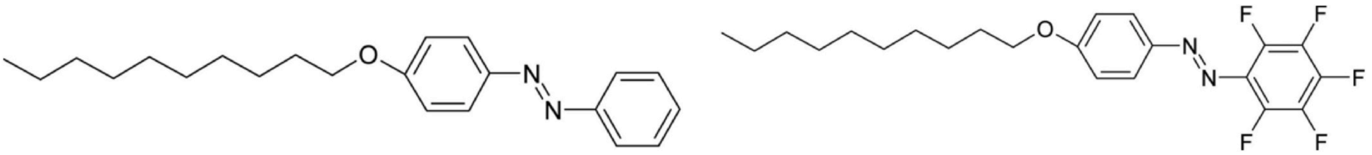

Fig. 7. Structures of the two different azobenzene molecules studied, 4-(decyloxy)azobenzene (left) and fluorinated 4-(decyloxy)azobenzene (right) in their trans conformation. Hydrogen atoms are not shown for clarity. Reproduced from Ref. [75] with permission of the American Chemical Society.

and CT mechanisms in the proximity of organic-organic interfaces has not yet been investigated in detail from computation, although fast exciton and charge transport in the interfacial region are essential to obtain efficient exciton-to-free-charge conversion. Few studies present in the literature consider QM/MM calculations on disordered C_{60} and p-type semiconductors small molecules interfaces obtained from MD simulations (Fig. 8) with different polarity to calculate the DOS and excitation energies [126–128].

Fast exciton transport is necessary to enable the exciton to reach the interface within its radiative lifetime whereas high carrier mobilities ensure rapid charge separation after the photoinduced CT step [129]. In this view, the authors of this study found that exciton and charge transport at the studied interfaces are disorder-limited [128]. The reduced packing density strongly affects the van der Waals interactions, which dominate the DOS distribution, but are state independent. In contrast, long-range polarization and electrostatic interactions are less affected by the packing density, but they differ for different states. In addition, electrostatic interactions cause an energetic spread of excitation energies as soon as molecules undergo a change in polarity upon electronic excitation, and the delocalization over dimers profoundly influences the DOS of excitonic states (Fig. 8). As a result, a given morphology might result in largely disordered polaronic and considerably less disordered excitonic states and vice versa.

A different donor-acceptor 0D-1D HNJ has been considered in a joint experimental-computational study by Harvey and coworkers, in which a GNR interacts with different pyrene-linked dyes through strong $\pi-\pi$ interactions, with pyrene used as probes to assess the photophysical changes observed upon the interface formation [130]. The authors identified three distinct cases: (1) non-harvesting CT, (2) harvesting and emissive CT, and (3) harvesting but non-emissive CT complexes (Fig. 9). The excitons of the GNR polymer are rapidly and fully channeled to the CT complex in less than 1 ps by an ET process.

By combining DFT optimization in the ground state and TD-DFT single point in the excite state, together with different experimental characterization, the authors observed that the photoinduced processes occur during the first 100 fs after generation of an exciton and this first step consists of an ET from the surroundings to a CT assembly that subsequently lead to charge generation. Interestingly, almost all excitons are harvested within a picosecond. Afterward, the photophysical behavior of this 0D-1D interface follows the prediction of the three-state theory, which includes a coupling between a local exciton (here the 0D material) and its CT state. The three extreme cases observed show that (1) a minimal driving force is required to form a full intermolecular CT state ($GNR^{+}-dye^{-}$); (2) low driving forces lead to a strong coupling between a local exciton and a CT state, and (3) a strong spectral overlap is a critical parameter for predicting the harvesting efficiency of a CT assembly, due to the "hidden" nature of the absorption bands within those of the donors and acceptors.

In a very recent work, a 0D-2D interface consisting of a perylene derivative (PTCDI) physisorbed on a free-standing graphene monolayer has been studied by DFT to assess the changes in electronic and optical properties of the HNJ [131]. The most interesting findings of this study is that the electrons follow the rules of the ordinary 2D materials for the charge conduction process, since the effective masses for both holes and electrons are only marginally changed due to the PTCDI adsorption, while the holes obey those of the 2D Dirac materials. From the CT

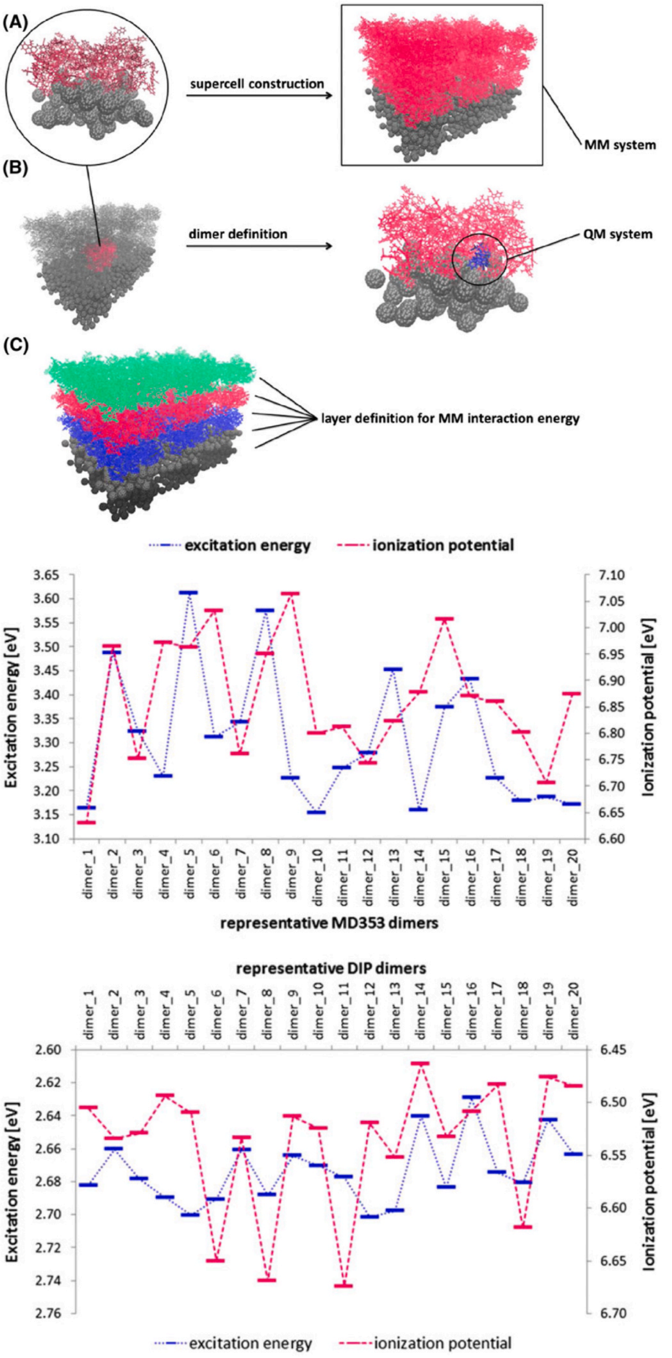

Fig. 8. Representation (top) of the computational approach considered in the study reported in Ref. [128]. Excitation energies (left, blue bars) and ionization potentials (pink bars) calculated for 20 randomly selected dimers of MD353 (upper panel) and DIP (lower panel) (bottom). Reproduced from Ref. [128] with permission of Wiley-VCH. (For interpretation of the references to color in this figure legend, the reader is referred to the Web version of this article.)

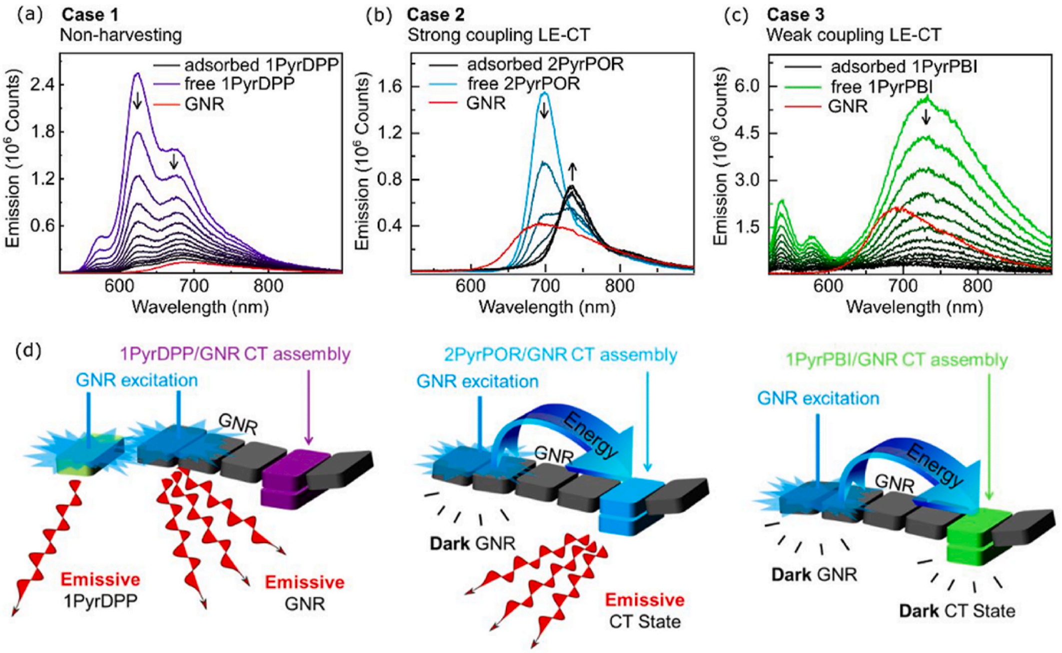

Fig. 9. CT processes in GNR-pyrene nanohybrids. Reproduced from Ref. [130] with permission of the American Chemical Society.

process, PTCDI gain electrons from the graphene, which demonstrate p-type doping attributes. The additional investigation of optical properties reveals that the optical response of the interface is anisotropic in nature.

The second important method to analyze ET/CT from computation is non-adiabatic molecular dynamics (NAMD) simulations, in which the evolution in time of the electron density is studied. Due to the high computational costs of this method, only small systems are commonly considered, and interfaces are limited to models of few hundred atoms. Yet, thanks to the development of high computing clusters in recent years, NAMD starts to become a powerful tool to assess both ET and CT of HNJs. One approach to overcome these difficulties is to design an appropriate simplified method. Density-functional tight binding (DFTB) has become a popular form of approximate density-functional theory based on a minimal valence basis set and neglect of all but two center integrals. DFTB is designed to behave like DFT, but with better scalability with respect to the number of atoms in the system (thanks to approximation methods from semi-empirical methods). In this view, it can be seen as an ‘approximate DFT’ since it is parameterized to fit DFT (rather than parameterized using experimental data).

Darghouth et al. [132] reported very recently the study of a pentacene/C60 0D-0D interface in which a long-range corrected (Rlc) time-dependent (TD) DFTB [133] has been used to carry out fewest switches surface hopping calculations [134]. As a result, the study found that the Rlc parameter is essential to obtain a proper description of both ET and CT mechanisms; small values of Rlc yields the condensed-phase CT time of about 100 fs, while ET and CT times strongly increase with larger Rlc values. This is backed up with the CT process $P^*/F \rightarrow P^+/F^-$ which shows that the initial transfer of electrons is accompanied by a partial delocalization of the hole over both fragments, which then re-localizes back onto P, consistent with a polaron-like picture in which the nuclei relax to stabilize the redistribution of charges.

In a different study, time-domain DFTB has been combined with NAMD to investigate both the ET and electrons-holes (e−h) recombination at a SWCNT/perylenediimide (SWCNT/PDI) 0D-1D interface [135]. The authors focus here on the role that defects on SWCNT play in the photoinduced excited-state dynamics. To achieve high efficiencies, ET should be fast, while subsequent charge recombination should be slow. Typically, defects are detrimental to material performance because they accelerate charge and energy losses. Yet, the authors demonstrated that defects in SWCNT improve the performance of both ET and CT processes. As a consequence, the defects lower the D-A energy gap for the photoinduced ET, the coupling becomes stronger and the ET rate increases as compared to the pristine system. These findings show the power of state-of-the-art NAMD computations, and to a wider extend, it can be foreseen that this phenomenon might apply also to other low-dimensional interfaces, since they can dissipate the strain induced by the defect better than bulk materials.

3.2. CNSs-based nanohybrids with inorganic NBBs

The integration methods for CNSs and inorganic NBBs into novel nanohybrids are divided into two categories according to the procedures of the synthesis namely *in-situ* and *ex-situ* strategies [136]. In the *in-situ* strategy, CNSs-inorganic NBBs nanoarchitectures are formed during the synthesis of the inorganic NBBs (or the CNSs) by adding the other NBB. A variety of synthesis methods have been applied to uniformly create inorganic NBBs on the surface of CNSs. More specifically, methodologies such as sol-gel processes [137–139], evaporation techniques [140,141], wet chemical processes [142,143], hydrothermal and aerosol techniques [144,145], chemical vapor deposition [146,147] and electrochemical deposition [148] have endowed the resulting hybrids with distinct morphologies, structures, sizes and properties. A variety of inorganic NBBs including metals [149], metal oxides [138,144,145], metal chalcogenides and perovskites [150,151] have been coupled this way to CNSs. On the basis of the *in-situ* strategy, the CNSs are suitable substrates for inorganic NBBs in most cases and no surface functionalization steps, which might influence other properties, are required to connect CNSs and the NBBs. As reported for some CNSs-inorganic NBBs systems, the CNSs can be employed as substrates not only to facilitate the growth of inorganic NBBs along specific directions, but also to dissipate the heat during the crystallization of the NBBs in order to control the morphology and structure or to shrink and homogenize the size of the NBBs [137].

The hybridization of two different NBBs after they have been synthesized is called *ex-situ* strategy [136]. This strategy relies on either covalent, non-covalent or electrostatic interactions between the CNSs and inorganic NBBs. Covalent approaches usually rely on the modification (or native presence) of oxygen containing groups on the surface of

CNSs or employ aryl diazonium-based direct arylation methods that target the CNS double bonds in order to construct covalent bonds with the organic ligands that protrude from the NBBs [4,152]. Fig. 10 shows an example in which SWCNTs were oxidized to yield terminal carboxylate groups, that also improves the solubility in N, N-dimethylformamide (DMF), and then reacted with cysteamine-protected CdS quantum dots (QDs), to generate covalent nanohybrids [153]. Thanks to this strong covalent bond, the SWCNTs can act as an electron acceptor to minimize the charge recombination in the CdS QDs when employed as photooxidation catalysts.

Non-covalent strategies make use of van der Waals or π–π interactions to efficiently connect CNSs with inorganic NBBs. In most cases, it is necessary to add ligands which tend to establish such interactions between the two NBBs. Ligands with the role of tuning the hydrophobicity/hydrophilicity properties in inorganic NBBs have been employed as linkers in the nanohybrids with CNSs. For instance, Brown et al. fabricated CdSe QDs capped with hydrophobic trioctylphosphine oxide (TOPO) and these ligands were capable of connecting the QDs with hydrophobic C60 in mixed solutions of toluene and acetonitrile [154]. The hydrophobic alkyl chains of tetraoctylammonium bromide (TOAB) interact with SWCNTs, creating hybrid HNJs with CdS QDs [155]. There are also reports about other ligands on the inorganic NBBs able to form non-covalent interactions with CNSs. For instance, Kim et al. reported graphene-PbS QDs layered HNJs with oleic acid as ligands in between [156]. The attachment of other CNSs like RGO to TOPO-capped CdSe QDs have also been described [157]. Besides, polymers can also behave as intermediates to connect CNSs and inorganic NBBs. Polypyrrole can cover silica beads to form a composite which is attractive for GQDs [158]. 2D transition metal dichalcogenides (TMDs) are coupled to CNSs to create van der Waals heterostructures. For example, graphene-MoS_2 [159], graphene-ReS_2 [160], graphene-WS_2 [161], graphene-$MoTe_2$ [162] heterostructures were fabricated via the stacking method. A GQDs-MoS_2 heterostructure was prepared by drop casting [163].

Efforts have also been devoted at modifying the surface of inorganic nanoparticles with ligands which contain aromatic rings and could provide π–π interactions with CNSs. For example, after tuning the surface ligands composition in plasmonic Au nanoparticles (AuNPs) with an alkylthiol-pyrene derivative, SWCNTs [95] and RGO [164] can be well-connected with AuNPs through π–π stacking, as displayed in Fig. 11a for the case of the nanotubes. The tight grafting and close proximity of the plasmonic AuNPs enable an ET process from the pyrene molecules to SWCNT (Fig. 11b), which does not take place when the AuNPs are not present, since no superposition between the pyrene PL and SWCNT absorption profile exists (resonance ET is not permitted and takes place thanks to the plasmonic effect of the particles).

NBBs with opposite charges on the surface are prone to attract each other and form electrostatic interactions. The binding of RGO to AuNPs can also be achieved through this mechanism [165]. CNSs can also be decorated with charged ligands that attract inorganic NBBs by electrostatic interactions. For instance, CdTe QDs stabilized with negatively charged thioglycolic acid associate with CNTs bearing cationic pyrene derivatives on the surface, to assemble into photo-active CNTs-CdTe nanohybrids [166].

In comparison with the *in-situ* strategy, the most apparent advantage of the *ex-situ* one is that the structure, size and morphology of both CNSs and inorganic NBBs are easier to control [136]. However for the *ex-situ* strategy, the functionalization of the NBBs is mandatory, otherwise the two different NBBs cannot attach each other due to the absence of active interacting points. The process of functionalization can bring the risk of destroying other properties of the involved nanomaterials.

Different CNSs-inorganic NBBs nanohybrids have been reported as promising materials in several optoelectronic applications such as solar cells, photodetectors, photoelectrochemistry and optical sensing. In the case of solar cells, nanohybrids with CNSs and inorganic NBBs were applied due to their interesting ability of hindering the electron-hole pair recombination. Within the nanohybrids, the inorganic NBBs are in charge of light absorption and charge separation, while the CNSs are generally used as efficient electron acceptors. The most notable nanohybrids in this field are CNSs-CdS QDs. The uniform distribution of QDs on the surface of SWCNTs enables a maximization of light absorption and charge collection. SWCNT-CdS hybrids showed an incident photon to current efficiency (IPCE) of 0.45%, which is anyway far away from industrial application [153]. An IPCE of up to 16% was reached through modification on the thickness and morphology of the light harvesting layers [167]. The investigation on other Cd chalcogenides-based hybrid systems has been carried out and IPCE values for, respectively, non-thiolated CNTs-CdSe, thiolated CNTs-CdSe, thiolated RGO-CdSe, fullerene-CdSe, stacked carbon nanocups-CdSe and CNTs-CdTe nanohybrids of 1.85% [157], 1.88% [157], 2.02% [157], 4.5% [155], 5% [155], and 2.3% [166] were recorded. Kim et al. reported a unique heterostructure based on graphene coupled to PbS QDs for extraction and transport of photogenerated charges with an IPCE of 6.36% [156]. Other than for the synergetic effect in improving the CT, the nanohybrids have been the focus of interest for their stability compared to the simple nanoparticles in photovoltaic devices [157].

The excellent PL properties of some inorganic NBBs in combination with the charge transport properties of CNSs can be used to build light-driven chemical sensors. As reported by Zor et al., by adding organic toxic compound tributyltin or other pesticides in a silica beads-poypyrrole-GQDs system, a quantitative relationship between the PL intensity of the nanohybrids and the amount of analytes can be recorded [158]. Due to the synergetic effect of the different parts within the nanohybrids, the sensing mechanism could be explained: silica beads with polypyrrole coverage separate and preconcentrate the analytes, while GQDs transduce illumination into optical signal which is dependent on the analyte binding. A SWCNTs-CdS QDs nanosystem was also reported as a chemical sensor for detecting oleylamine [168]. Differently from the silica beads-GQDs system, inorganic CdS nanoparticles act as charge separator under illumination and n-type conducting

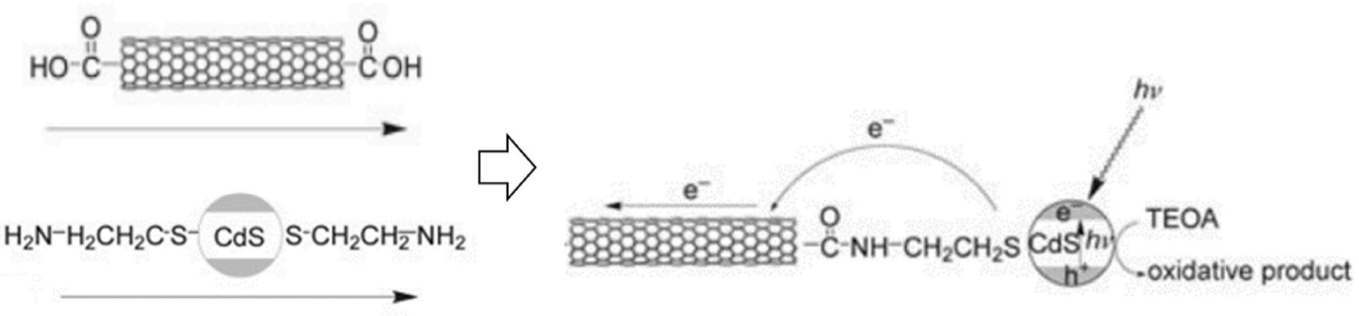

Fig. 10. Covalent hybridization of oxidized SWCNTs with CdS QDs to favor a photo-activated oxidation process of organic molecules. Reproduced from Ref. [153] with permission of Wiley-VCH.

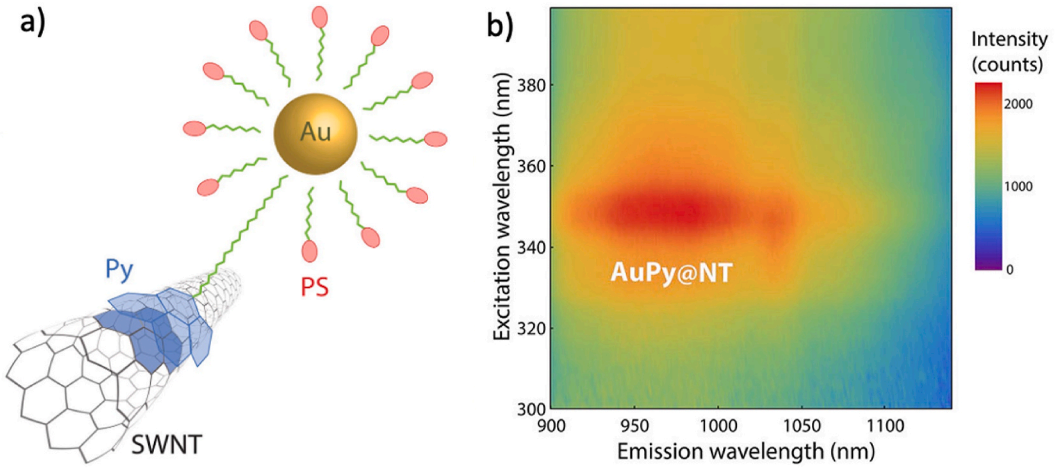

Fig. 11. a) Non-covalent nanohybrids between pyrene-functionalized AuNPs and SWCNTs in which photo-induced ET between pyrene molecules and SWCNTs is enabled by the presence of the plasmonic AuNPs, as shown in the PL excitation/emission map in b). Adapted from Ref. [95] with permission of Wiley-VCH.

properties are enhanced when the amount of oleylamine is increased. The reversible signal is detected from the photocurrent through a photoelectrochemical method (Fig. 12).

The optical and electrical properties of the CNSs-inorganic NBBs HNJs open up also new opportunities for the fabrication of photodetectors. RGO-CdSe QDs nanohybrids were used as photodetector species and were found to have different response times in different atmosphere, namely NO_2 > air > N_2 > NH_3 [169]. These results can be interpreted considering that the energy levels of CdSe QDs are bent at the RGO/QDs interface due to gas adsorption. One of the classic combinations is that of CNSs with 2D TMDs. For example, a GQD-MoS_2 nanohybrid showed broad-spectra light detection ranging from UV to NIR [163]. The band gap of the GQDs allows response in the UV and visible, while the response in the visible/NIR light is due to MoS_2. Moreover, the difference in the Fermi levels between the GQDs and MoS_2 facilitates a charge separation process under visible illumination, which enhances response for visible light. A graphene/WS_2 photodetector displayed a responsivity of 950 A W^{-1} and a rise time of 7.85 s [161]. A graphene-$MoTe_2$ photodetector showed a responsivity of 970.82 A W^{-1} at 1064 nm and a response rate of 78 ms [162]. A graphene-ReS_2 photodetector showed a photoresponsivity of 7×10^5 A W^{-1}, a detectivity of 1.9×10^{13} Jones and a fast response time of less than 30 ms [160]. A glassy graphene-MoS_2 photodetector exhibited a responsivity of 12.3 mA W^{-1} under the illumination of 532 nm [159].

Metal halide perovskites are also incorporated in nanohybrids to yield effective photodetection. A nanocrystalline graphite-$MAPbI_3$ nanohybrid was employed as photodetector for visible light detection [151]. Higher photocurrent and shorter delay time than the neat $MAPbI_3$ were obtained with the nanohybrid, proving an improvement in optoelectronic properties. A graphene-$MAPbI_3$ hybrid sample was studied as photodetector with a broad spectral photoresponsivity between 800 and 400 nm due to an increase in the optical absorption and the occurrence of a photogating mechanisms in the hybrid system compared to the bare perovskite [170]. In a newest report, a graphene-$MAPbI_3$ heterostructure was employed as flexible image sensor [150]. In such hybrid system, electrons from graphene are transferred to the empty valence band produced through photon absorption in the $MAPbI_3$ perovskite, thus resulting in a reduction in recombination of photoexcited electron-hole pairs in $MAPbI_3$ to obtain a high photoresponsivity, (~10^7 A/W), low operating voltage (0.1 V), and low response time (less than 50 ms).

In the field of photoelectrochemistry, CNSs-based nanohybrids can play the role of electrode materials for efficient CT: in a photoelectrochemical cell, it is indeed very likely that the presence of CNSs induces an efficient CT pathway [171]. Photocatalysis shares a similar mechanism. The presence of photogenerated species in inorganic semiconducting NBBs can drive photocatalytic reactions, while the CNSs can generally accelerate the CT and minimize the charge recombination

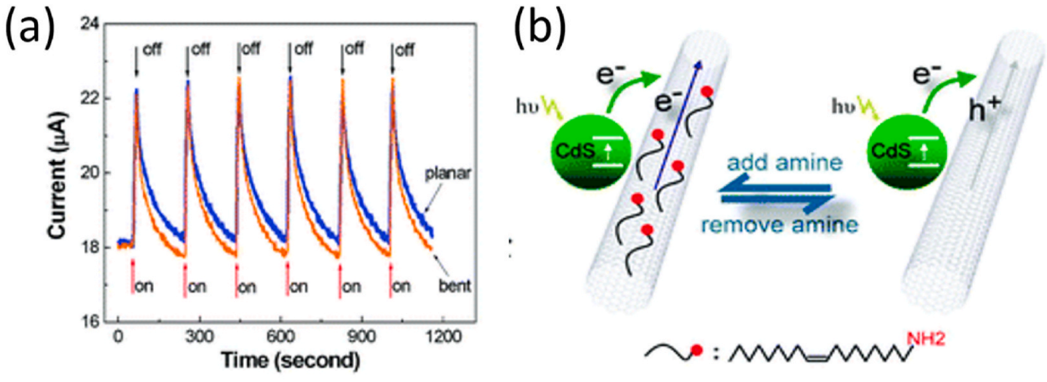

Fig. 12. a) Reproducible current change with time in responding to illumination of nanohybrid films of SWCNTs-CdS QDs transferred onto a PET substrate. The curves were measured when the PET film was in a planar (blue curve) or bent (orange curve) state. b) Model showing light-driven chemical-sensing process when an analyte (e.g., oleylamine) is added to or removed from the nanohybrid system. Note: e− and h + represent electron and hole, respectively. Adapted from Ref. [168] with permission of the American Chemical Society. (For interpretation of the references to color in this figure legend, the reader is referred to the Web version of this article.)

[172]. CNSs-inorganic NBBs nanohybrids emerge as a growing and promising group of photocatalysts, with some examples including GQDs-ZnO [145], polymeric graphitic carbon nitride-$Bi_4Ti_3O_{12}$/$Bi_2Ti_2O_7$ [173] and CNTs-TiO_2 or RGO-TiO_2 [174]. Besides, more and more CNSs-inorganic NBBs hybrid systems are developed and proved to exhibit highly efficient CT, such as CNTs-Ta_2O_5, [138] CNTs-CdSe@ZnS [152], RGO-Ag [175], or GO-CdTe [176]. These systems are promising in a lot of fields where light-energy conversion is required, including photovoltaics, photoelectrochemistry/photocatalysis and sensing.

4. Conclusion and outlook

Special features of nanocarbons make them suitable for optoelectronic applications: 1) the atomic layer thickness ensures transparency and flexibility, which is benefit for integration in windows or portable/wearable devices; 2) the quantum domain leads to strong excitonic binding effects and improves light absorption efficiency; 3) the bandgaps are closely related to active layers thicknesses and thus the optical absorption wavelength range and can be modulated by tuning the size and geometry of the assembly and the dimensions of the individual NBBs [23]. Although GBMs have the above advantages, most of them have narrow absorption bands and poor light absorption, while the large-scale preparation of high-quality single crystals is still a great challenge. In contrast, 0D and 1D materials have advantages of broad absorption bandwidth, high absorption efficiency, flexibility, light weight and ease of processing. By combining the advantages of these CNSs, the constructed HNJs with other NBBs may exhibit the properties that are not available in any single material, and it is expected the obtainment of high performance in both absorption and emission to promote the development of a new generation of optoelectronic devices [136].

Despite the amazing potential of such low-dimensional HNJs, some fundamental aspects are still unclear, and in particular it is relevant to proceed judiciously with respect to the following aspects, when willing to design new CNS-based HNJs:

1) how to choose suitable NBBs to combine them to achieve optimal performance. For instance, to build a type I or II HNJ, the first choice of a SMOS or GQD is to consider whether its HOMO-LUMO can be properly matched with the energy levels of a 1D or 2D material as outlined previously (Fig. 3). The characteristics of the HNJ interface affect the interfacial electronic structure. For example, GQDs have excellent tunable absorption, but tend to aggregate in solution, making their use limited. On the other hand, for the GQDs functionalized with SMOSs or hybridized with 1/2D materials the aggregation can be strongly suppressed, and their properties can be finely tuned in the direction of photo-induced ET/CT;
2) how to design a high-quality interface of different low-dimensional materials. The interface between 2D and 0D/1D NBBs controls both the ET and CT processes. A fine tuning of the frontier energy levels is thus required and can be assessed by use of rational design, taking for example advantage of the predictive power of computation;
3) how the structure of the nano-assembly affects the interface properties. It is not trivial to obtain an efficient CT or ET at an interface, since morphology can play an important role and the energy tuning alone can be not sufficient to assess the proper outcome. For example, a 0D NBB can assembly in different ways on a 2D material, and to gain control of the different possible players for an efficient ET/CT at the interface, different control levels on these hybrid assemblies have to be considered as well as different key parameters have to be tuned, such as the distance, the tilting angle, the density and the position of the NBBs within the identified HNJ. Augmented control over geometry and symmetry in complex nano-hybrids is expected to be able to reveal novel interesting properties which will pave the way to new exciting applications.

By considering all these aspects, it will be possible to proceed many steps ahead in the design and assembly of nanocarbons-based HNJs with other photo-active nanomaterials, significantly improving the response of the individual NBBs. Special attention should be also devoted to resort to low-cost materials, based on environmentally friendly, earth-abundant and non-toxic elements, to which also the additional cost benefit delivered by low-temperature wet chemical processing from “green” solvents shall be added, enabling the realization of future sustainable optoelectronic devices that will be integrated in many contests of our everyday lives.

CRediT authorship contribution statement

Silvio Osella: Writing – original draft, Writing – review & editing. **Mengjiao Wang:** Writing – original draft. **Enzo Menna:** Writing – original draft, Writing – review & editing. **Teresa Gatti:** Supervision, Writing – original draft, Writing – review & editing.

Declaration of competing interest

The authors declare that they have no known competing financial interests or personal relationships that could have appeared to influence the work reported in this paper.

Acknowledgements

S.O. thanks the Polish National Science Centre for funding (grant no. UMO-2018/31/D/ST4/01475) and the Polish National Agency for Academic Exchange under the Bekker program (grant no. PPN/BEK/2020/1/00053/U/00001). M. W. and T.G. would like to thank the Hessisches Ministerium für Wissenschaft und Kunst (HMWK) for financial support through the Hessen Horizon Program with a Marie Skłodowska-Curie-Stipendium Hessen assigned to M.W. after the obtainment of the MSCA 2020 Seal of Excellence from the European Commission for the project NANOHYLUM. T.G. acknowledges financial support from the European Commission with the H2020 FET-PROACTIVE-EIC-07-2020 project LIGHT-CAP (project number 101017821) and from the Deutsche Forschungsgemeinschaft (DFG) with the project C-LINKNANO (GA 3052/1-1). E.M. would like to thank “Centro Studi di Economia e Tecnica dell'Energia Giorgio Levi Cases” (project PRINTERS) and Department of Chemical Sciences (project P-DISC#06BIRD2019-UNIPD) of the University of Padova for financial support.

References

[1] M. Zeng, Y. Zhang, Colloidal nanoparticle inks for printing functional devices: emerging trends and future prospects, J. Mater. Chem. A. 7 (2019) 23301–23336, https://doi.org/10.1039/C9TA07552F.

[2] N. Zhao, L. Yan, X. Zhao, X. Chen, A. Li, D. Zheng, X. Zhou, X. Dai, F.-J. Xu, Versatile types of organic/inorganic nanohybrids: from strategic design to biomedical applications, Chem. Rev. 119 (2019) 1666–1762, https://doi.org/10.1021/acs.chemrev.8b00401.

[3] G. Guan, M.-Y. Han, Functionalized hybridization of 2D nanomaterials, Adv. Sci. 6 (2019) 1901837, https://doi.org/10.1002/advs.201901837.

[4] T. Gatti, N. Vicentini, M. Mba, E. Menna, Organic functionalized carbon nanostructures for functional polymer-based nanocomposites, Eur. J. Org. Chem. 2016 (2016) 1071–1090, https://doi.org/10.1002/ejoc.201501411.

[5] S. Lee, M.-J. Choi, G. Sharma, M. Biondi, B. Chen, S.-W. Baek, A.M. Najarian, M. Vafaie, J. Wicks, L.K. Sagar, S. Hoogland, F.P.G. de Arquer, O. Voznyy, E. H. Sargent, Orthogonal colloidal quantum dot inks enable efficient multilayer optoelectronic devices, Nat. Commun. 11 (2020) 4814, https://doi.org/10.1038/s41467-020-18655-7.

[6] G. Hu, J. Kang, L.W.T. Ng, X. Zhu, R.C.T. Howe, C.G. Jones, M.C. Hersam, T. Hasan, Functional inks and printing of two-dimensional materials, Chem. Soc. Rev. 47 (2018) 3265–3300, https://doi.org/10.1039/C8CS00084K.

[7] V. Balzani, Nanoscience and nanotechnology: the bottom-up construction of molecular devices and machines, Pure Appl. Chem. 80 (2008) 1631–1650, https://doi.org/10.1351/pac200880081631.

[8] S. Zhang, Building from the bottom up, Mater. Today 6 (2003) 20–27, https://doi.org/10.1016/S1369-7021(03)00530-3.

[9] J. Gao, H. Wang, Q. Yuan, Y. Feng, Structure and function of the photosystem supercomplexes, Front. Plant Sci. 9 (2018) 357, https://doi.org/10.3389/fpls.2018.00357.

[10] L. Himanen, A. Geurts, A.S. Foster, P. Rinke, Data-driven materials science: status, challenges, and perspectives, Adv. Sci. 6 (2019) 1900808, https://doi.org/10.1002/advs.201900808.

[11] Y. Hong, B. Hou, H. Jiang, J. Zhang, Machine learning and artificial neural network accelerated computational discoveries in materials science, WIREs Comput. Mol. Sci. 10 (2020), e1450, https://doi.org/10.1002/wcms.1450.

[12] D. Jariwala, V.K. Sangwan, L.J. Lauhon, T.J. Marks, M.C. Hersam, Carbon nanomaterials for electronics, optoelectronics, photovoltaics, and sensing, Chem. Soc. Rev. 42 (2013) 2824–2860, https://doi.org/10.1039/C2CS35335K.

[13] Z. Zhang, L. Wei, X. Qin, Y. Li, Carbon nanomaterials for photovoltaic process, Nano Energy 15 (2015) 490–522, https://doi.org/10.1016/j.nanoen.2015.04.003.

[14] V. Schroeder, S. Savagatrup, M. He, S. Lin, T.M. Swager, Carbon nanotube chemical sensors, Chem. Rev. 119 (2019) 599–663, https://doi.org/10.1021/acs.chemrev.8b00340.

[15] L. Wieland, H. Li, C. Rust, J. Chen, B.S. Flavel, Carbon nanotubes for photovoltaics: from lab to industry, Adv. Energy Mater. 11 (2021) 2002880, https://doi.org/10.1002/aenm.202002880.

[16] M. Bacon, S.J. Bradley, T. Nann, Graphene quantum dots, Part. Part. Syst. Char. 31 (2014) 415–428, https://doi.org/10.1002/ppsc.201300252.

[17] C. Anichini, P. Samorì, Graphene-based hybrid functional materials, Small (2021) 2100514, https://doi.org/10.1002/smll.202100514, n/a.

[18] A. Stergiou, N. Tagmatarchis, Interfacing carbon dots for charge-transfer processes, Small (2021) 2006005, https://doi.org/10.1002/smll.202006005, n/a.

[19] D.M. Guldi, R.D. Costa, Nanocarbon hybrids: the paradigm of nanoscale self-ordering/self-assembling by means of charge transfer/doping interactions, J. Phys. Chem. Lett. 4 (2013) 1489–1501, https://doi.org/10.1021/jz4001714.

[20] C.J. Shearer, A. Cherevan, D. Eder, Application and future challenges of functional nanocarbon hybrids, Adv. Mater. 26 (2014) 2295–2318, https://doi.org/10.1002/adma.201305254.

[21] Y. Zhan, Y. Mei, L. Zheng, Materials capability and device performance in flexible electronics for the Internet of Things, J. Mater. Chem. C. 2 (2014) 1220–1232, https://doi.org/10.1039/C3TC31765J.

[22] M.H. Miraz, M. Ali, P.S. Excell, R. Picking, Internet of nano-things, things and everything: future growth trends, Future Internet 10 (2018), https://doi.org/10.3390/fi10080068.

[23] C.J. Shearer, L. Yu, J.G. Shapter, Optoelectronic properties of nanocarbons and nanocarbon films, Synth. Appl. Nanocarbons. (2020) 275–294, https://doi.org/10.1002/9781119429418.ch9.

[24] F. Bonaccorso, Z. Sun, T. Hasan, A.C. Ferrari, Graphene photonics and optoelectronics, Nat. Photonics 4 (2010) 611–622, https://doi.org/10.1038/nphoton.2010.186.

[25] S. Nanot, E.H. Hároz, J.-H. Kim, R.H. Hauge, J. Kono, Optoelectronic properties of single-wall carbon nanotubes, Adv. Mater. 24 (2012) 4977–4994, https://doi.org/10.1002/adma.201201751.

[26] P. Avouris, M. Freitag, V. Perebeinos, Carbon-nanotube photonics and optoelectronics, Nat. Photonics 2 (2008) 341–350, https://doi.org/10.1038/nphoton.2008.94.

[27] P. Tian, L. Tang, K.S. Teng, S.P. Lau, Graphene quantum dots from chemistry to applications, Mater. Today Chem. 10 (2018) 221–258, https://doi.org/10.1016/j.mtchem.2018.09.007.

[28] M. Ozhukil Valappil, V.K. Pillai, S. Alwarappan, Spotlighting graphene quantum dots and beyond: synthesis, properties and sensing applications, Appl. Mater. Today. 9 (2017) 350–371, https://doi.org/10.1016/j.apmt.2017.09.002.

[29] G.M. Paternò, Q.Chen Goudappagouda, F. G. Lanzani, A. Narita Scotognella, Large polycyclic aromatic hydrocarbons as graphene quantum dots: from synthesis to spectroscopy and photonics, Adv. Opt. Mater. n/a (2021) 2100508, https://doi.org/10.1002/adom.202100508.

[30] N. Javed, D.M. O'Carroll, Carbon dots and stability of their optical properties, Part. Part. Syst. Char. 38 (2021) 2000271, https://doi.org/10.1002/ppsc.202000271.

[31] A. Privitera, M. Righetto, D. Mosconi, F. Lorandi, A.A. Isse, A. Moretto, R. Bozio, C. Ferrante, L. Franco, Boosting carbon quantum dots/fullerene electron transfer via surface group engineering, Phys. Chem. Chem. Phys. 18 (2016) 31286–31295, https://doi.org/10.1039/C6CP05981C.

[32] S. Osella, S. Knippenberg, Environmental effects on the charge transfer properties of Graphene quantum dot based interfaces, Int. J. Quant. Chem. 119 (2019), e25882, https://doi.org/10.1002/qua.25882.

[33] M. Semeniuk, Z. Yi, V. Poursorkhabi, J. Tjong, S. Jaffer, Z.-H. Lu, M. Sain, Future perspectives and review on organic carbon dots in electronic applications, ACS Nano 13 (2019) 6224–6255, https://doi.org/10.1021/acsnano.9b00688.

[34] M. Takase, T. Narita, W. Fujita, M.S. Asano, T. Nishinaga, H. Benten, K. Yoza, K. Müllen, Pyrrole-fused Azacoronene family: the influence of replacement with dialkoxybenzenes on the optical and electronic properties in neutral and oxidized states, J. Am. Chem. Soc. 135 (2013) 8031–8040, https://doi.org/10.1021/ja402371f.

[35] E. Gońka, P.J. Chmielewski, T. Lis, M. Stępień, Expanded hexapyrrolohexaazacoronenes. Near-infrared absorbing chromophores with interrupted peripheral conjugation, J. Am. Chem. Soc. 136 (2014) 16399–16410, https://doi.org/10.1021/ja508963v.

[36] A. Privitera, M. Righetto, D. Mosconi, F. Lorandi, A.A. Isse, A. Moretto, R. Bozio, C. Ferrante, L. Franco, Boosting carbon quantum dots/fullerene electron transfer via surface group engineering, Phys. Chem. Chem. Phys. 18 (2016) 31286–31295, https://doi.org/10.1039/C6CP05981C.

[37] S. Miao, K. Liang, J. Zhu, B. Yang, D. Zhao, B. Kong, Hetero-atom-doped carbon dots: doping strategies, properties and applications, Nano Today 33 (2020) 100879, https://doi.org/10.1016/j.nantod.2020.100879.

[38] W.A. Gaviria Rojas, M.C. Hersam, Chirality-enriched carbon nanotubes for next-generation computing, Adv. Mater. 32 (2020) 1905654, https://doi.org/10.1002/adma.201905654.

[39] F. Yang, M. Wang, D. Zhang, J. Yang, M. Zheng, Y. Li, Chirality pure carbon nanotubes: growth, sorting, and characterization, Chem. Rev. 120 (2020) 2693–2758, https://doi.org/10.1021/acs.chemrev.9b00835.

[40] A.S.R. Bati, L. Yu, M. Batmunkh, J.G. Shapter, Synthesis, purification, properties and characterization of sorted single-walled carbon nanotubes, Nanoscale 10 (2018) 22087–22139, https://doi.org/10.1039/C8NR07379A.

[41] S.K. Samanta, M. Fritsch, U. Scherf, W. Gomulya, S.Z. Bisri, M.A. Loi, Conjugated polymer-assisted dispersion of single-wall carbon nanotubes: the power of polymer wrapping, Acc. Chem. Res. 47 (2014) 2446–2456, https://doi.org/10.1021/ar500141j.

[42] F.J. Berger, J. Lüttgens, T. Nowack, T. Kutsch, S. Lindenthal, L. Kistner, C. C. Müller, L.M. Bongartz, V.A. Lumsargis, Y. Zakharko, J. Zaumseil, Brightening of long, polymer-wrapped carbon nanotubes by sp3 functionalization in organic solvents, ACS Nano 13 (2019) 9259–9269, https://doi.org/10.1021/acsnano.9b03792.

[43] A.H. Brozena, M. Kim, L.R. Powell, Y. Wang, Controlling the optical properties of carbon nanotubes with organic colour-centre quantum defects, Nat. Rev. Chem. 3 (2019) 375–392, https://doi.org/10.1038/s41570-019-0103-5.

[44] X. He, H. Htoon, S.K. Doorn, W.H.P. Pernice, F. Pyatkov, R. Krupke, A. Jeantet, Y. Chassagneux, C. Voisin, Carbon nanotubes as emerging quantum-light sources, Nat. Mater. 17 (2018) 663–670, https://doi.org/10.1038/s41563-018-0109-2.

[45] A.H. Brozena, J.D. Leeds, Y. Zhang, J.T. Fourkas, Y. Wang, Controlled defects in semiconducting carbon nanotubes promote efficient generation and luminescence of trions, ACS Nano 8 (2014) 4239–4247, https://doi.org/10.1021/nn500894p.

[46] Y. Piao, B. Meany, L.R. Powell, N. Valley, H. Kwon, G.C. Schatz, Y. Wang, Brightening of carbon nanotube photoluminescence through the incorporation of sp3 defects, Nat. Chem. 5 (2013) 840–845, https://doi.org/10.1038/nchem.1711.

[47] A. Hirsch, Functionalization of single-walled carbon nanotubes, Angew. Chem. Int. Ed. 41 (2002) 1853–1859, https://doi.org/10.1002/1521-3773(20020603)41:11<1853::AID-ANIE1853>3.0.CO;2-N.

[48] D. Tasis, N. Tagmatarchis, A. Bianco, M. Prato, Chemistry of carbon nanotubes, Chem. Rev. 106 (2006) 1105–1136, https://doi.org/10.1021/cr050569o.

[49] V. Saraswat, R.M. Jacobberger, M.S. Arnold, Materials science challenges to graphene nanoribbon electronics, ACS Nano 15 (2021) 3674–3708, https://doi.org/10.1021/acsnano.0c07835.

[50] A. Narita, X. Feng, K. Müllen, Bottom-up synthesis of chemically precise graphene nanoribbons, Chem. Rec. 15 (2015) 295–309, https://doi.org/10.1002/tcr.201402082.

[51] S. Osella, A. Narita, M.G. Schwab, Y. Hernandez, X. Feng, K. Müllen, D. Beljonne, Graphene nanoribbons as low band gap donor materials for organic photovoltaics: quantum chemical aided design, ACS Nano 6 (2012) 5539–5548, https://doi.org/10.1021/nn301478c.

[52] Z. Chen, A. Narita, K. Müllen, Graphene nanoribbons: on-surface synthesis and integration into electronic devices, Adv. Mater. 32 (2020) 2001893, https://doi.org/10.1002/adma.202001893.

[53] V. Saraswat, R.M. Jacobberger, M.S. Arnold, Materials science challenges to graphene nanoribbon electronics, ACS Nano 15 (2021) 3674–3708, https://doi.org/10.1021/acsnano.0c07835.

[54] Y. Hu, P. Xie, M. De Corato, A. Ruini, S. Zhao, F. Meggendorfer, L.A. Straasø, L. Rondin, P. Simon, J. Li, J.J. Finley, M.R. Hansen, J.-S. Lauret, E. Molinari, X. Feng, J.V. Barth, C.-A. Palma, D. Prezzi, K. Müllen, A. Narita, Bandgap engineering of graphene nanoribbons by control over structural distortion, J. Am. Chem. Soc. 140 (2018) 7803–7809, https://doi.org/10.1021/jacs.8b02209.

[55] L. Yang, C.-H. Park, Y.-W. Son, M.L. Cohen, S.G. Louie, Quasiparticle energies and band gaps in graphene nanoribbons, Phys. Rev. Lett. 99 (2007) 186801, https://doi.org/10.1103/PhysRevLett.99.186801.

[56] K. Wakabayashi, K. Sasaki, T. Nakanishi, T. Enoki, Electronic states of graphene nanoribbons and analytical solutions, Sci. Technol. Adv. Mater. 11 (2010) 54504, https://doi.org/10.1088/1468-6996/11/5/054504.

[57] Y. Hu, P. Xie, M. De Corato, A. Ruini, S. Zhao, F. Meggendorfer, L.A. Straasø, L. Rondin, P. Simon, J. Li, J.J. Finley, M.R. Hansen, J.-S. Lauret, E. Molinari, X. Feng, J.V. Barth, C.-A. Palma, D. Prezzi, K. Müllen, A. Narita, Bandgap engineering of graphene nanoribbons by control over structural distortion, J. Am. Chem. Soc. 140 (2018) 7803–7809, https://doi.org/10.1021/jacs.8b02209.

[58] V. Singh, D. Joung, L. Zhai, S. Das, S.I. Khondaker, S. Seal, Graphene based materials: past, present and future, Prog. Mater. Sci. 56 (2011) 1178–1271, https://doi.org/10.1016/j.pmatsci.2011.03.003.

[59] K.S. Novoselov, A.K. Geim, S.V. Morozov, D. Jiang, Y. Zhang, S.V. Dubonos, I. V. Grigorieva, A.A. Firsov, Electric field effect in atomically thin carbon films, Science (306) (2004) 666, https://doi.org/10.1126/science.1102896. LP – 66 80.

[60] K.S. Novoselov, A. Mishchenko, A. Carvalho, A.H. Castro Neto, 2D materials and van der Waals heterostructures, Science 353 (2016) aac9439, https://doi.org/10.1126/science.aac9439, 80.

[61] A. McCreary, O. Kazakova, D. Jariwala, Z.Y. Al Balushi, An outlook into the flat land of 2D materials beyond graphene: synthesis, properties and device applications, 2D Mater. 8 (2020) 13001, https://doi.org/10.1088/2053-1583/abc13d.

[62] H.-X. Wang, Q. Wang, K.-G. Zhou, H.-L. Zhang, Graphene in light: design, synthesis and applications of photo-active graphene and graphene-like materials, Small 9 (2013) 1266–1283, https://doi.org/10.1002/smll.201203040.

[63] J. Singh, H.E. Ruda, M.R. Narayan, D. Ompong, Concept of excitons, Opt. Prop. Mater. Their Appl. (2019) 129–155, https://doi.org/10.1002/9781119506003.ch5.

[64] V. Strauss, A. Roth, M. Sekita, D.M. Guldi, Efficient energy-conversion materials for the future: understanding and tailoring charge-transfer processes in carbon nanostructures, Chem 1 (2016) 531–556, https://doi.org/10.1016/j.chempr.2016.09.001.

[65] T. Gatti, E. Menna, Use of carbon nanostructures in hybrid photovoltaic devices, in: Photoenergy Thin Film Mater, John Wiley & Sons, Inc., Hoboken, NJ, USA, 2019, pp. 1–47, https://doi.org/10.1002/9781119580546.ch1.

[66] A. Zampetti, A. Minotto, F. Cacialli, Near-infrared (NIR) organic light-emitting diodes (OLEDs): challenges and opportunities, Adv. Funct. Mater. 29 (2019) 1807623, https://doi.org/10.1002/adfm.201807623.

[67] A. Graf, C. Murawski, Y. Zakharko, J. Zaumseil, M.C. Gather, Infrared organic light-emitting diodes with carbon nanotube emitters, Adv. Mater. 30 (2018) 1706711, https://doi.org/10.1002/adma.201706711.

[68] X. He, H. Htoon, S.K. Doorn, W.H.P. Pernice, F. Pyatkov, R. Krupke, A. Jeantet, Y. Chassagneux, C. Voisin, Carbon nanotubes as emerging quantum-light sources, Nat. Mater. 17 (2018) 663–670, https://doi.org/10.1038/s41563-018-0109-2.

[69] A.H. Brozena, J.D. Leeds, Y. Zhang, J.T. Fourkas, Y. Wang, Controlled defects in semiconducting carbon nanotubes promote efficient generation and luminescence of trions, ACS Nano 8 (2014) 4239–4247, https://doi.org/10.1021/nn500894p.

[70] A.H. Brozena, M. Kim, L.R. Powell, Y. Wang, Controlling the optical properties of carbon nanotubes with organic colour-centre quantum defects, Nat. Rev. Chem. 3 (2019) 375–392, https://doi.org/10.1038/s41570-019-0103-5.

[71] W. Niu, J. Ma, P. Soltani, W. Zheng, F. Liu, A.A. Popov, J.J. Weigand, H. Komber, E. Poliani, C. Casiraghi, J. Droste, M.R. Hansen, S. Osella, D. Beljonne, M. Bonn, H.I. Wang, X. Feng, J. Liu, Y. Mai, A curved graphene nanoribbon with multi-edge structure and high intrinsic charge carrier mobility, J. Am. Chem. Soc. 142 (2020) 18293–18298, https://doi.org/10.1021/jacs.0c07013.

[72] X. Yao, W. Zheng, S. Osella, Z. Qiu, S. Fu, D. Schollmeyer, B. Müller, D. Beljonne, M. Bonn, H.I. Wang, K. Müllen, A. Narita, Synthesis of nonplanar graphene nanoribbon with Fjord edges, J. Am. Chem. Soc. 143 (2021) 5654–5658, https://doi.org/10.1021/jacs.1c01882.

[73] Z. Liu, H. Qiu, C. Wang, Z. Chen, B. Zyska, A. Narita, A. Ciesielski, S. Hecht, L. Chi, K. Müllen, P. Samorì, Photomodulation of charge transport in all-semiconducting 2D–1D van der Waals heterostructures with suppressed persistent photoconductivity effect, Adv. Mater. 32 (2020) 2001268, https://doi.org/10.1002/adma.202001268.

[74] M. Döbbelin, A. Ciesielski, S. Haar, S. Osella, M. Bruna, A. Minoia, L. Grisanti, T. Mosciatti, F. Richard, E.A. Prasetyanto, L. De Cola, V. Palermo, R. Mazzaro, V. Morandi, R. Lazzaroni, A.C. Ferrari, D. Beljonne, P. Samorì, Light-enhanced liquid-phase exfoliation and current photoswitching in graphene–azobenzene composites, Nat. Commun. 7 (2016) 11090, https://doi.org/10.1038/ncomms11090.

[75] S. Osella, A. Minoia, D. Beljonne, Combined molecular dynamics and density functional theory study of azobenzene–graphene interfaces, J. Phys. Chem. C 120 (2016) 6651–6658, https://doi.org/10.1021/acs.jpcc.6b00393.

[76] M. Gobbi, S. Bonacchi, J.X. Lian, A. Vercouter, S. Bertolazzi, B. Zyska, M. Timpel, R. Tatti, Y. Olivier, S. Hecht, M.V. Nardi, D. Beljonne, E. Orgiu, P. Samorì, Collective molecular switching in hybrid superlattices for light-modulated two-dimensional electronics, Nat. Commun. 9 (2018) 2661, https://doi.org/10.1038/s41467-018-04932-z.

[77] X. Zhang, L. Hou, P. Samorì, Coupling carbon nanomaterials with photochromic molecules for the generation of optically responsive materials, Nat. Commun. 7 (2016) 11118, https://doi.org/10.1038/ncomms11118.

[78] D. Tasis, N. Tagmatarchis, A. Bianco, M. Prato, Chemistry of carbon nanotubes, Chem. Rev. 106 (2006) 1105–1136, https://doi.org/10.1021/cr050569o.

[79] V. Georgakilas, M. Otyepka, A.B. Bourlinos, V. Chandra, N. Kim, K.C. Kemp, P. Hobza, R. Zboril, K.S. Kim, Functionalization of graphene: covalent and non-covalent approaches, derivatives and applications, Chem. Rev. 112 (2012) 6156–6214, https://doi.org/10.1021/cr3000412.

[80] T. Gatti, G. Girardi, N. Vicentini, R. Brandiele, M. Wirix, C. Durante, E. Menna, Physico-chemical, electrochemical and structural insights into poly(3,4-ethylenedioxythiophene) grafted from molecularly engineered multi-walled carbon nanotube surfaces, J. Nanosci. Nanotechnol. 18 (2018) 1006–1018, https://doi.org/10.1166/jnn.2018.15250.

[81] T. Gatti, F. Lamberti, P. Topolovsek, M. Abdu-Aguye, R. Sorrentino, L. Perino, M. Salerno, L. Girardi, C. Marega, G.A. Rizzi, M.A. Loi, A. Petrozza, E. Menna, Interfacial morphology addresses performance of perovskite solar cells based on composite hole transporting materials of functionalized reduced graphene oxide and P3HT, Sol. RRL. 2 (2018) 1800013, https://doi.org/10.1002/solr.201800013.

[82] T. Gatti, S. Casaluci, M. Prato, M. Salerno, F. Di Stasio, A. Ansaldo, E. Menna, A. Di Carlo, F. Bonaccorso, Boosting perovskite solar cells performance and stability through doping a poly-3(hexylthiophene) hole transporting material with organic functionalized carbon nanostructures, Adv. Funct. Mater. 26 (2016), https://doi.org/10.1002/adfm.201602803.

[83] M. D'Este, M. De Nardi, E. Menna, A Co-functionalization approach to soluble and functional single-walled carbon nanotubes, Eur. J. Org Chem. 2006 (2006) 2517–2522, https://doi.org/10.1002/ejoc.200600196.

[84] F. Cordella, M. De Nardi, E. Menna, C. Hébert, M.A. Loi, Tuning the photophysical properties of soluble single-wall carbon nanotube derivatives by co-functionalization with organic molecules, Carbon N. Y. 47 (2009) 1264–1269, https://doi.org/10.1016/j.carbon.2009.01.004.

[85] T. Gatti, N. Manfredi, C. Boldrini, F. Lamberti, A. Abbotto, E. Menna, A D-π-A organic dye – reduced graphene oxide covalent dyad as a new concept photosensitizer for light harvesting applications, Carbon N. Y. 115 (2017), https://doi.org/10.1016/j.carbon.2017.01.081.

[86] P. Guarracino, T. Gatti, N. Canever, M. Abdu-Aguye, M.A. Loi, E. Menna, L. Franco, Probing photoinduced electron-transfer in graphene-dye hybrid materials for DSSC, Phys. Chem. Chem. Phys. 19 (2017) 27716–27724, https://doi.org/10.1039/c7cp04308b.

[87] C. Di Berardino, P. Bélteky, F. Schmitz, F. Lamberti, E. Menna, Á. Kukovecz, T. Gatti, Controlled size reduction of liquid exfoliated graphene micro-sheets via tip sonication, Cryst 10 (2020), https://doi.org/10.3390/cryst10111049.

[88] A.M. Ross, M. Zheng, M. Maggini, F. Marangi, G. Cerullo, T. Gatti, F. Scotognella, Revealing excited states dynamics in cross-linked covalent hybrids of graphene and diketopyrrolopyrrole oligomers via ultrafast transient absorption spectroscopy, EPJ Web Conf. 238 (2020), https://doi.org/10.1051/epjconf/202023807007.

[89] M. Zheng, F. Lamberti, L. Franco, E. Collini, I. Fortunati, G. Bottaro, G. Daniel, R. Sorrentino, A. Minotto, A. Kukovecz, E. Menna, S. Silvestrini, C. Durante, F. Cacialli, G. Meneghesso, M. Maggini, T. Gatti, A film-forming graphene/diketopyrrolopyrrole covalent hybrid with far-red optical features: evidence of photo-stability, Synth. Met. 258 (2019) 116201, https://doi.org/10.1016/j.synthmet.2019.116201.

[90] P. Salice, P. Maity, E. Rossi, T. Carofiglio, E. Menna, M. Maggini, The continuous-flow cycloaddition of azomethine ylides to carbon nanotubes, Chem. Commun. 47 (2011) 9092–9094, https://doi.org/10.1039/C1CC13155A.

[91] P. Salice, C. Sartorio, A. Burlini, R. Improta, B. Pignataro, E. Menna, On the trade-off between processability and opto-electronic properties of single wall carbon nanotube derivatives in thin film heterojunctions, J. Mater. Chem. C. 3 (2015) 303–312, https://doi.org/10.1039/C4TC01350F.

[92] B.W. Smith, M. Monthioux, D.E. Luzzi, Encapsulated C60 in carbon nanotubes, Nature 396 (1998) 323–324, https://doi.org/10.1038/24521.

[93] P. Salice, A. Gambarin, N. Daldosso, F. Mancin, E. Menna, Noncovalent interaction between single-walled carbon nanotubes and pyrene-functionalized gold nanoparticles in water-soluble nanohybrids, J. Phys. Chem. C 118 (2014) 27028–27038, https://doi.org/10.1021/jp505005e.

[94] C. Sartorio, V. Figà, P. Salice, D. Gragnato, S. Cataldo, M. Scopelliti, R. Improta, E. Menna, B. Pignataro, Thiophene pyrenyl derivatives for the supramolecular processability of single-walled carbon nanotubes in thin film heterojunction, Synth. Met. 229 (2017) 7–15, https://doi.org/10.1016/j.synthmet.2017.04.018.

[95] M. Glaeske, S. Juergensen, L. Gabrielli, E. Menna, F. Mancin, T. Gatti, A. Setaro, Plasmon-Assisted energy transfer in hybrid nanosystems, Phys. Status Solidi Rapid Res. Lett. 12 (2018), https://doi.org/10.1002/pssr.201800508.

[96] M. Yudasaka, K. Ajima, K. Suenaga, T. Ichihashi, A. Hashimoto, S. Iijima, Nano-extraction and nano-condensation for C60 incorporation into single-wall carbon nanotubes in liquid phases, Chem. Phys. Lett. 380 (2003) 42–46, https://doi.org/10.1016/j.cplett.2003.08.095.

[97] A.N. Khlobystov, D.A. Britz, J. Wang, S.A. O'Neil, M. Poliakoff, G.A.D. Briggs, Low temperature assembly of fullerene arrays in single-walled carbon nanotubes using supercritical fluids, J. Mater. Chem. 14 (2004) 2852–2857, https://doi.org/10.1039/B404167D.

[98] J. Gao, P. Blondeau, P. Salice, E. Menna, B. Bártová, C. Hébert, J. Leschner, U. Kaiser, M. Milko, C. Ambrosch-Draxl, M.A. Loi, Electronic interactions between "pea" and "pod": the case of oligothiophenes encapsulated in carbon nanotubes, Small 7 (2011) 1807–1815, https://doi.org/10.1002/smll.201100319.

[99] M.A. Loi, J. Gao, F. Cordella, P. Blondeau, E. Menna, B. Bártová, C. Hébert, S. Lazar, G.A. Botton, M. Milko, C. Ambrosch-Draxl, Encapsulation of conjugated oligomers in single-walled carbon nanotubes: towards nanohybrids for photonic devices, Adv. Mater. 22 (2010) 1635–1639, https://doi.org/10.1002/adma.200903527.

[100] K. Yanagi, H. Kataura, Breaking Kasha's rule, Nat. Photonics 4 (2010) 200–201, https://doi.org/10.1038/nphoton.2010.77.

[101] M. Milko, P. Puschnig, P. Blondeau, E. Menna, J. Gao, M.A. Loi, C. Draxl, Evidence of hybrid excitons in weakly interacting nanopeapods, J. Phys. Chem. Lett. 4 (2013) 2664–2667, https://doi.org/10.1021/jz401073t.

[102] A. Cadena, B. Botka, E. Székely, K. Kamarás, Encapsulation of sexithiophene molecules in single-walled carbon nanotubes using supercritical CO2 at low temperature, Phys. Status Solidi 257 (2020) 2000314, https://doi.org/10.1002/pssb.202000314.

[103] M. Kalbáč, L. Kavan, S. Gorantla, T. Gemming, L. Dunsch, Sexithiophene encapsulated in a single-walled carbon nanotube: an in situ Raman spectroelectrochemical study of a peapod structure, Chem. Eur J. 16 (2010) 11753–11759, https://doi.org/10.1002/chem.201001417.

[104] N.S. Mueller, S. Heeg, P. Kusch, E. Gaufrès, N.Y.-W. Tang, U. Hübner, R. Martel, A. Vijayaraghavan, S. Reich, Plasmonic enhancement of SERS measured on molecules in carbon nanotubes, Faraday Discuss 205 (2017) 85–103, https://doi.org/10.1039/C7FD00127D.

[105] S. Wasserroth, S. Heeg, N.S. Mueller, P. Kusch, U. Hübner, E. Gaufrès, N.Y.-W. Tang, R. Martel, A. Vijayaraghavan, S. Reich, Resonant, plasmonic Raman enhancement of α-6T molecules encapsulated in carbon nanotubes, J. Phys. Chem. C 123 (2019) 10578–10585, https://doi.org/10.1021/acs.jpcc.9b01600.

[106] R.S. Alencar, A.L. Aguiar, R.S. Ferreira, R. Chambard, B. Jousselme, J.-L. Bantignies, C. Weigel, S. Clément, R. Aznar, D. Machon, A.G. Souza Filho, A. San-Miguel, L. Alvarez, Raman resonance tuning of quaterthiophene in filled

carbon nanotubes at high pressures, Carbon N. Y. 173 (2021) 163–173, https://doi.org/10.1016/j.carbon.2020.10.083.

[107] Y. Almadori, L. Alvarez, R. Le Parc, R. Aznar, F. Fossard, A. Loiseau, B. Jousselme, S. Campidelli, P. Hermet, A. Belhboub, A. Rahmani, T. Saito, J.-L. Bantignies, Chromophore ordering by confinement into carbon nanotubes, J. Phys. Chem. C 118 (2014) 19462–19468, https://doi.org/10.1021/jp505804d.

[108] Y. Almadori, G. Delport, R. Chambard, L. Orcin-Chaix, A.C. Selvati, N. Izard, A. Belhboub, R. Aznar, B. Jousselme, S. Campidelli, P. Hermet, R. Le Parc, T. Saito, Y. Sato, K. Suenaga, P. Puech, J.S. Lauret, G. Cassabois, J.-L. Bantignies, L. Alvarez, Fermi level shift in carbon nanotubes by dye confinement, Carbon N. Y. 149 (2019) 772–780, https://doi.org/10.1016/j.carbon.2019.04.041.

[109] A. Belhboub, P. Hermet, L. Alvarez, R. Le Parc, S. Rols, A.C. Lopes Selvati, B. Jousselme, Y. Sato, K. Suenaga, A. Rahmani, J.-L. Bantignies, Enhancing the infrared response of carbon nanotubes from oligo-quaterthiophene interactions, J. Phys. Chem. C 120 (2016) 28802–28807, https://doi.org/10.1021/acs.jpcc.6b09329.

[110] B.M. C. J, R.A.H. F. B, R.A. C. H, Raman analysis of conjugated bithiophene (2T) encapsulated in semiconducting and metallic single-walled carbon nanotubes, J. Raman Spectrosc. 51 (2020) 1315–1323, https://doi.org/10.1002/jrs.5903.

[111] J. Chenouf, M. Boutahir, A. Rahmani, H. Chadli, P. Hermet, J. Mejía-López, A. Rahmani, Charge transfer evidence in donor–acceptor single-walled carbon nanotubes filled with sexithiophene oligomers: nanotube diameter dependence, J. Raman Spectrosc. n/a (2021), https://doi.org/10.1002/jrs.6139.

[112] K. Miyaura, Y. Miyata, B. Thendie, K. Yanagi, R. Kitaura, Y. Yamamoto, S. Arai, H. Kataura, H. Shinohara, Extended-conjugation π-electron systems in carbon nanotubes, Sci. Rep. 8 (2018) 8098, https://doi.org/10.1038/s41598-018-26379-4.

[113] T. Yumura, H. Yamashita, Modulating the electronic properties of multimeric thiophene oligomers by utilizing carbon nanotube confinement, J. Phys. Chem. C 118 (2014) 5510–5522, https://doi.org/10.1021/jp5006555.

[114] T. Fujimori, K. Urita, Red-emitting Ͽ-conjugated oligomers infused single-wall carbon nanotube sheets, Chem. Phys. Lett. 649 (2016) 53–59, https://doi.org/10.1016/j.cplett.2016.02.041.

[115] M. Tange, T. Okazaki, Z. Liu, K. Suenaga, S. Iijima, Room-temperature Y-type emission of perylenes by encapsulation within single-walled carbon nanotubes, Nanoscale 8 (2016) 7834–7839, https://doi.org/10.1039/C5NR08578K.

[116] T. Koyama, T. Tsunekawa, T. Saito, K. Asaka, Y. Saito, H. Kishida, A. Nakamura, Synthesis and photophysics of quaterrylene molecules in single-walled carbon nanotubes: excitation energy transfer between a nanoscale cylinder and encapsulated molecules, J. Phys. Chem. C 118 (2014) 21671–21681, https://doi.org/10.1021/jp506361b.

[117] J. Campo, Y. Piao, S. Lam, C.M. Stafford, J.K. Streit, J.R. Simpson, A.R. Hight Walker, J.A. Fagan, Enhancing single-wall carbon nanotube properties through controlled endohedral filling, Nanoscale Horizons 1 (2016) 317–324, https://doi.org/10.1039/C6NH00062B.

[118] A. Nakamura, K. Yamanaka, K. Miyaura, H.E. Lim, K. Matsuda, B. Thendie, Y. Miyata, T. Kochi, S. Okada, H. Shinohara, Ultrafast charge transfer and relaxation dynamics in polymer-encapsulating single-walled carbon nanotubes: polythiophene and coronene polymer, J. Phys. Chem. C 122 (2018) 16940–16949, https://doi.org/10.1021/acs.jpcc.8b03757.

[119] S. van Bezouw, D.H. Arias, R. Ihly, S. Cambré, A.J. Ferguson, J. Campo, J. C. Johnson, J. Defillet, W. Wenseleers, J.L. Blackburn, Diameter-dependent optical absorption and excitation energy transfer from encapsulated dye molecules toward single-walled carbon nanotubes, ACS Nano 12 (2018) 6881–6894, https://doi.org/10.1021/acsnano.8b02213.

[120] T. Yumura, W. Yamamoto, Kinetic control in the alignment of polar π-conjugated molecules inside carbon nanotubes, J. Phys. Chem. C 122 (2018) 18151–18160, https://doi.org/10.1021/acs.jpcc.8b05455.

[121] S. Osella, M. Kiliszek, E. Harputlu, C.G. Unlu, K. Ocakoglu, J. Kargul, B. Trzaskowski, Controlling the charge transfer flow at the graphene/pyrene–nitrilotriacetic acid interface, J. Mater. Chem. C. 6 (2018) 5046–5054, https://doi.org/10.1039/C8TC00564H.

[122] S. Osella, M. Kiliszek, E. Harputlu, C.G. Unlu, K. Ocakoglu, B. Trzaskowski, J. Kargul, Role of metal centers in tuning the electronic properties of graphene-based conductive interfaces, J. Phys. Chem. C 123 (2019) 8623–8632, https://doi.org/10.1021/acs.jpcc.9b00170.

[123] P. Cudazzo, L. Sponza, C. Giorgetti, L. Reining, F. Sottile, M. Gatti, Exciton band structure in two-dimensional materials, Phys. Rev. Lett. 116 (2016) 66803, https://doi.org/10.1103/PhysRevLett.116.066803.

[124] H. Wang, W. Liu, X. He, P. Zhang, X. Zhang, Y. Xie, An excitonic perspective on low-dimensional semiconductors for photocatalysis, J. Am. Chem. Soc. 142 (2020) 14007–14022, https://doi.org/10.1021/jacs.0c06966.

[125] M.C. Scharber, N.S. Sariciftci, Efficiency of bulk-heterojunction organic solar cells, Prog. Polym. Sci. 38 (2013) 1929–1940, https://doi.org/10.1016/j.progpolymsci.2013.05.001.

[126] C. Brückner, F. Würthner, K. Meerholz, B. Engels, Atomistic approach to simulate processes relevant for the efficiencies of organic solar cells as a function of molecular properties. II. Kinetic aspects, J. Phys. Chem. C 121 (2017) 26–51, https://doi.org/10.1021/acs.jpcc.6b11340.

[127] C. Brückner, F. Würthner, K. Meerholz, B. Engels, Structure–property relationships from atomistic multiscale simulations of the relevant processes in organic solar cells. I. Thermodynamic aspects, J. Phys. Chem. C 121 (2017) 4–25, https://doi.org/10.1021/acs.jpcc.6b06755.

[128] C. Brückner, M. Stolte, F. Würthner, J. Pflaum, B. Engels, QM/MM calculations combined with the dimer approach on the static disorder at organic-organic interfaces of thin-film organic solar cells composed of small molecules, J. Phys. Org. Chem. 30 (2017), e3740, https://doi.org/10.1002/poc.3740.

[129] P.K. Nayak, K.L. Narasimhan, D. Cahen, Separating charges at organic interfaces: effects of disorder, hot states, and electric field, J. Phys. Chem. Lett. 4 (2013) 1707–1717, https://doi.org/10.1021/jz4002339.

[130] L. Tanguy, A. Fleury, P.-L. Karsenti, G. Brisard, A. Soldera, P.D. Harvey, Ultrafast energy transfer from local exciton to intermolecular CT states in a supramolecular model of the donor–acceptor interfaces, J. Phys. Chem. C 124 (2020) 16248–16260, https://doi.org/10.1021/acs.jpcc.0c02381.

[131] S. Sinha, S. Ghosal, D. Jana, Electronic and optical properties of PTCDI adsorbed graphene heterostructure: a first principles study, J. Phys. Chem. Solid. 155 (2021) 110109, https://doi.org/10.1016/j.jpcs.2021.110109.

[132] A.A.M.H.M. Darghouth, M.E. Casida, X. Zhu (朱熹), B. Natarajan, H. Su (蘇海斌), A. Humeniuk, E. Titov, X. Miao (缪昕丞), R. Mitrić, Effect of varying the TD-lc-DFTB range-separation parameter on charge and energy transfer in a model pentacene/buckminsterfullerene heterojunction, J. Chem. Phys. 154 (2021) 54102, https://doi.org/10.1063/5.0024559.

[133] A. Humeniuk, R. Mitrić, Long-range correction for tight-binding TD-DFT, J. Chem. Phys. 143 (2015) 134120, https://doi.org/10.1063/1.4931179.

[134] A. Humeniuk, R. Mitrić, DFTBaby: a software package for non-adiabatic molecular dynamics simulations based on long-range corrected tight-binding TD-DFT(B), Comput, Phys. Commun. 221 (2017) 174–202, https://doi.org/10.1016/j.cpc.2017.08.012.

[135] R. Sarkar, M. Kar, M. Habib, G. Zhou, T. Frauenheim, P. Sarkar, S. Pal, O. V. Prezhdo, Common defects accelerate charge separation and reduce recombination in CNT/molecule composites: atomistic quantum dynamics, J. Am. Chem. Soc. 143 (2021) 6649–6656, https://doi.org/10.1021/jacs.1c02325.

[136] C.J. Shearer, A. Cherevan, D. Eder, Application and future challenges of functional nanocarbon hybrids, Adv. Mater. 26 (2014) 2295–2318, https://doi.org/10.1002/adma.201305254.

[137] D. Eder, A.H. Windle, Morphology control of CNT-TiO2 hybrid materials and rutile nanotubes, J. Mater. Chem. 18 (2008) 2036–2043, https://doi.org/10.1039/B800499D.

[138] A.S. Cherevan, D. Eder, Dual excitation transient photocurrent measurement for charge transfer studies in nanocarbon hybrids and composites, Adv. Mater. Interfaces. 3 (2016) 1600244, https://doi.org/10.1002/admi.201600244.

[139] Y. Li, B.-P. Zhang, J.-X. Zhao, Z.-H. Ge, X.-K. Zhao, L. Zou, ZnO/carbon quantum dots heterostructure with enhanced photocatalytic properties, Appl. Surf. Sci. 279 (2013) 367–373, https://doi.org/10.1016/j.apsusc.2013.04.114.

[140] R.-J. Chung, Z.-C. Lin, P.-K. Yang, K.-Y. Lai, S.-F. Jen, P.-W. Chiu, Hybrid ZnO NR/graphene structures as advanced optoelectronic devices with high transmittance, Nanoscale Res. Lett. 8 (2013) 350, https://doi.org/10.1186/1556-276X-8-350.

[141] J. Yang, X. Zhao, X. Shan, H. Fan, L. Yang, Y. Zhang, X. Li, Blue-shift of UV emission in ZnO/graphene composites, J. Alloys Compd. 556 (2013) 1–5, https://doi.org/10.1016/j.jallcom.2012.12.098.

[142] A. Sett, D. Das, D. Banerjee, U.K. Ghorai, N.S. Das, B. Das, K.K. Chattopadhyay, 1D–2D hybrids as efficient optoelectronic materials: a study on graphitic carbon nitride nanosheets wrapped with zinc oxide rods, Dalton Trans. 47 (2018) 4501–4507, https://doi.org/10.1039/C8DT00016F.

[143] X. Qin, Q. Li, A.M. Asiri, A.O. Al-Youbi, X. Sun, One-pot synthesis of Au nanoparticles/reduced graphene oxide nanocomposites and their application for electrochemical H2O2, glucose, and hydrazine sensing, Gold Bull. 47 (2014) 3–8, https://doi.org/10.1007/s13404-013-0094-9.

[144] H. Bozetine, Q. Wang, A. Barras, M. Li, T. Hadjersi, S. Szunerits, R. Boukherroub, Green chemistry approach for the synthesis of ZnO–carbon dots nanocomposites with good photocatalytic properties under visible light, J. Colloid Interface Sci. 465 (2016) 286–294, https://doi.org/10.1016/j.jcis.2015.12.001.

[145] H. Yu, H. Zhang, H. Huang, Y. Liu, H. Li, H. Ming, Z. Kang, ZnO/carbon quantum dots nanocomposites: one-step fabrication and superior photocatalytic ability for toxic gas degradation under visible light at room temperature, New J. Chem. 36 (2012) 1031–1035, https://doi.org/10.1039/C2NJ20959D.

[146] J. Yi, J.M. Lee, W. Il Park, Vertically aligned ZnO nanorods and graphene hybrid architectures for high-sensitive flexible gas sensors, Sensor. Actuator. B Chem. 155 (2011) 264–269, https://doi.org/10.1016/j.snb.2010.12.033.

[147] C. Wu, T.W. Kim, T. Guo, F. Li, Unique visible-light-assisted field emission of tetrapod-shaped ZnO/reduced graphene-oxide core/coating nanocomposites, Sci. Rep. 6 (2016) 38613, https://doi.org/10.1038/srep38613.

[148] Z. Yin, S. Wu, X. Zhou, X. Huang, Q. Zhang, F. Boey, H. Zhang, Electrochemical deposition of ZnO nanorods on transparent reduced graphene oxide electrodes for hybrid solar cells, Small 6 (2010) 307–312, https://doi.org/10.1002/smll.200901968.

[149] P. Tian, L. Tang, K.S. Teng, S.P. Lau, Graphene quantum dots from chemistry to applications, Mater. Today Chem. 10 (2018) 221–258, https://doi.org/10.1016/j.mtchem.2018.09.007.

[150] K. Xia, W. Wu, M. Zhu, X. Shen, Z. Yin, H. Wang, S. Li, M. Zhang, H. Wang, H. Lu, A. Pan, C. Pan, Y. Zhang, CVD growth of perovskite/graphene films for high-performance flexible image sensor, Sci. Bull. 65 (2020) 343–349, https://doi.org/10.1016/j.scib.2019.12.015.

[151] Y. Wang, Z. Xia, S. Du, F. Yuan, Z. Li, Z. Li, Q. Dai, H. Wang, S. Luo, S. Zhang, H. Zhou, Solution-processed photodetectors based on organic–inorganic hybrid perovskite and nanocrystalline graphite, Nanotechnology 27 (2016) 175201, https://doi.org/10.1088/0957-4484/27/17/175201.

[152] F. Mammeri, A. Ballarin, M. Giraud, G. Brusatin, S. Ammar, Photoluminescent properties of new quantum dot nanoparticles/carbon nanotubes hybrid structures, Colloids Surfaces A Physicochem. Eng. Asp. 439 (2013) 138–144, https://doi.org/10.1016/j.colsurfa.2013.03.026.

[153] L. Sheeney-Haj-Ichia, B. Basnar, I. Willner, Efficient generation of photocurrents by using CdS/carbon nanotube Assemblies on electrodes, Angew. Chem. Int. Ed. 44 (2005) 78–83, https://doi.org/10.1002/anie.200461666.

[154] P. Brown, P.V. Kamat, Quantum dot solar cells. Electrophoretic deposition of CdSe−C60 composite films and capture of photogenerated electrons with nC60 cluster shell, J. Am. Chem. Soc. 130 (2008) 8890–8891, https://doi.org/10.1021/ja802810c.

[155] I. Robel, B.A. Bunker, P.V. Kamat, Single-walled carbon nanotube–CdS nanocomposites as light-harvesting assemblies: photoinduced charge-transfer interactions, Adv. Mater. 17 (2005) 2458–2463, https://doi.org/10.1002/adma.200500418.

[156] B.-S. Kim, D.C.J. Neo, B. Hou, J.B. Park, Y. Cho, N. Zhang, J. Hong, S. Pak, S. Lee, J.I. Sohn, H.E. Assender, A.A.R. Watt, S. Cha, J.M. Kim, High performance PbS quantum dot/graphene hybrid solar cell with efficient charge extraction, ACS Appl. Mater. Interfaces 8 (2016) 13902–13908, https://doi.org/10.1021/acsami.6b02544.

[157] A.F. Madsuha, C. Van Pham, R. Thomann, M. Krueger, Quantum dot-nanocarbon based hybrid solar cells with improved long-term performance, Synth. Met. 222 (2016) 34–41, https://doi.org/10.1016/j.synthmet.2016.06.013.

[158] E. Zor, E. Morales-Narváez, A. Zamora-Gálvez, H. Bingol, M. Ersoz, A. Merkoçi, Graphene quantum dots-based photoluminescent sensor: a multifunctional composite for pesticide detection, ACS Appl. Mater. Interfaces 7 (2015) 20272–20279, https://doi.org/10.1021/acsami.5b05838.

[159] H. Xu, X. Han, X. Dai, W. Liu, J. Wu, J. Zhu, D. Kim, G. Zou, K.A. Sablon, A. Sergeev, Z. Guo, H. Liu, High detectivity and transparent few-layer MoS2/glassy-graphene heterostructure photodetectors, Adv. Mater. 30 (2018) 1706561, https://doi.org/10.1002/adma.201706561.

[160] B. Kang, Y. Kim, W.J. Yoo, C. Lee, Ultrahigh photoresponsive device based on ReS2/graphene heterostructure, Small 14 (2018) 1802593, https://doi.org/10.1002/smll.201802593.

[161] C. Lan, C. Li, S. Wang, T. He, Z. Zhou, D. Wei, H. Guo, H. Yang, Y. Liu, Highly responsive and broadband photodetectors based on WS2–graphene van der Waals epitaxial heterostructures, J. Mater. Chem. C. 5 (2017) 1494–1500, https://doi.org/10.1039/C6TC05037A.

[162] W. Yu, S. Li, Y. Zhang, W. Ma, T. Sun, J. Yuan, K. Fu, Q. Bao, Near-infrared photodetectors based on MoTe2/graphene heterostructure with high responsivity and flexibility, Small 13 (2017) 1700268, https://doi.org/10.1002/smll.201700268.

[163] P. Sahatiya, S.S. Jones, S. Badhulika, 2D MoS2–carbon quantum dot hybrid based large area, flexible UV–vis–NIR photodetector on paper substrate, Appl. Mater. Today. 10 (2018) 106–114, https://doi.org/10.1016/j.apmt.2017.12.013.

[164] L. Gabrielli, G. Altoè, M. Glaeske, S. Juergensen, S. Reich, A. Setaro, E. Menna, F. Mancin, T. Gatti, Controlling the decoration of the reduced graphene oxide surface with pyrene-functionalized gold nanoparticles, Phys. Status Solidi B 254 (2017) 1700281, 10.1002/pssb.201700281.

[165] D.-K. Lim, A. Barhoumi, R.G. Wylie, G. Reznor, R.S. Langer, D.S. Kohane, Enhanced photothermal effect of plasmonic nanoparticles coated with reduced graphene oxide, Nano Lett. 13 (2013) 4075–4079, https://doi.org/10.1021/nl4014315.

[166] D.M. Guldi, G.M.A. Rahman, V. Sgobba, N.A. Kotov, D. Bonifazi, M. Prato, CNT−CdTe versatile Donor−Acceptor nanohybrids, J. Am. Chem. Soc. 128 (2006) 2315–2323, https://doi.org/10.1021/ja0550733.

[167] C.X. Guo, H.B. Yang, Z.M. Sheng, Z.S. Lu, Q.L. Song, C.M. Li, Layered graphene/quantum dots for photovoltaic devices, Angew. Chem. Int. Ed. 49 (2010) 3014–3017, https://doi.org/10.1002/anie.200906291.

[168] X. Li, Y. Jia, A. Cao, Tailored single-walled carbon Nanotube−CdS nanoparticle hybrids for tunable optoelectronic devices, ACS Nano 4 (2010) 506–512, https://doi.org/10.1021/nn901757s.

[169] K. Yu, G. Lu, S. Mao, K. Chen, H. Kim, Z. Wen, J. Chen, Selective deposition of CdSe nanoparticles on reduced graphene oxide to understand photoinduced charge transfer in hybrid nanostructures, ACS Appl. Mater. Interfaces 3 (2011) 2703–2709, https://doi.org/10.1021/am200494v.

[170] Y. Lee, J. Kwon, E. Hwang, C.-H. Ra, W.J. Yoo, J.-H. Ahn, J.H. Park, J.H. Cho, High-performance perovskite–graphene hybrid photodetector, Adv. Mater. 27 (2015) 41–46, https://doi.org/10.1002/adma.201402271.

[171] J. Prakash, U. Prasad, R. Alexander, J. Bahadur, K. Dasgupta, A.N.M. Kannan, Photoelectrochemical solar water splitting: the role of the carbon nanomaterials in bismuth vanadate composite photoanodes toward efficient charge separation and transport, Langmuir 35 (2019) 14492–14504, https://doi.org/10.1021/acs.langmuir.9b02782.

[172] N. Syed, J. Huang, Y. Feng, X. Wang, L. Cao, Carbon-based nanomaterials via heterojunction serving as photocatalyst, Front. Chem. . 7 (2019) 713. https://www.frontiersin.org/article/10.3389/fchem.2019.00713.

[173] Y. Zhao, H. Fan, K. Fu, L. Ma, M. Li, J. Fang, Intrinsic electric field assisted polymeric graphitic carbon nitride coupled with Bi4Ti3O12/Bi2Ti2O7 heterostructure nanofibers toward enhanced photocatalytic hydrogen evolution, Int. J. Hydrogen Energy 41 (2016) 16913–16926, https://doi.org/10.1016/j.ijhydene.2016.07.162.

[174] L.M. Pastrana-Martínez, S. Morales-Torres, S.K. Papageorgiou, F.K. Katsaros, G. E. Romanos, J.L. Figueiredo, J.L. Faria, P. Falaras, A.M.T. Silva, Photocatalytic behaviour of nanocarbon–TiO2 composites and immobilization into hollow fibres, Appl. Catal. B Environ. 142–143 (2013) 101–111, https://doi.org/10.1016/j.apcatb.2013.04.074.

[175] J. Tian, S. Liu, Y. Zhang, H. Li, L. Wang, Y. Luo, A.M. Asiri, A.O. Al-Youbi, X. Sun, Environmentally friendly, one-pot synthesis of Ag nanoparticle-decorated reduced graphene oxide composites and their application to photocurrent generation, Inorg. Chem. 51 (2012) 4742–4746, https://doi.org/10.1021/ic300332x.

[176] A.M. Jagtap, V. Varade, B. Konkena, K.P. Ramesh, A. Chatterjee, A. Banerjee, N. B. Pendyala, K.S.R. Koteswara Rao, Interactions between photoexcited NIR emitting CdHgTe quantum dots and graphene oxide, J. Appl. Phys. 119 (2016) 74306, https://doi.org/10.1063/1.4942018.